https://doi.org/10.5194/egusphere-2026-108
Preprint. Discussion started: 15 January 2026
© Author(s) 2026. CC BY 4.0 License.

Spatial heterogeneity of sedimentary organic carbon in fjords around Stavanger, Norway – implications for upscaling

Markus Diesing[1], Reidulv Bøe[1], Sigrid Elvenes[1], Jochen Knies[1,2], Craig Smeaton[3]

[1]Geological Survey of Norway, Trondheim, Norway
[2]iC3: Centre for ice, Cryosphere, Carbon and Climate, Department of Geosciences, UiT The Arctic University of Norway, Tromsø, Norway
[3]School of Geography and Sustainable Development, University of St Andrews, St Andrews, United Kingdom

Correspondence to: Markus Diesing (markus.diesing@ngu.no)

Abstract. Fjords are steep sided glacially carved troughs that have been inundated by the sea. Several global assessments have aimed to establish the role of fjords in the carbon cycle. According to these studies, fjords bury 18 Tg of organic carbon per year, 55% to 62% of that organic carbon is terrestrially sourced and 61 ± 16% of the organic carbon in fjord sediments is thermally labile. Such quantitative estimates, while important for understanding the role of fjords in the global carbon cycle, often rest on data compilations that might not be representative for fjord environments as a whole and assumptions that might not hold. To test such assumptions, we present a local case study from fjords around Stavanger (Norway). Based on detailed investigations, we show that the seabed is heterogeneous in terms of substrate types covering the full grain-size spectrum from mud to boulders. Seabed areas where fine-grained sediment, and hence organic carbon, accumulates account for 50% of the area while the remainder is characterised by coarse-grained sediment indicating erosion and transport. In depositional areas, rates of organic carbon accumulation vary between 18.7 g m^{-2} yr^{-1} and 82.6 g m^{-2} yr^{-1} and stocks from 0.1 kg m^{-2} and 1.37 kg m^{-2}. The fraction of labile organic matter varies between 19% and 44%, while $\delta^{13}C$-values of the organic carbon fraction range from -27.44‰ to -21.23‰, indicating a strong variability of the sources of organic carbon over a comparatively small area. Taken together, these results attest to high environmental variability and spatial heterogeneity in the study site, putting several assumptions used in global assessments into question. We suggest steps to achieve more realistic results when upscaling from local studies to a higher level. Using available data on organic carbon accumulation rates from Norwegian coastal areas, we demonstrate how local results could be upscaled in a more robust way. We arrive at a tentative estimate of 0.41 – 3.68 Tg yr^{-1} of organic carbon accumulating in surface sediments (upper 10 cm) of fjords in mainland Norway.

1 Introduction

Fjords (also known as fiords, lochs and loughs) are over-deepened, mid to high-latitude estuaries which have been, or are presently being, excavated or modified by land-based ice (Howe et al., 2010; Syvitski et al., 1987). Globally, fjords cover an area of 445,859 km^2 according to Dürr et al. (2011) or 258,899 km^2 following a more recent estimate by Laruelle et al.

https://doi.org/10.5194/egusphere-2026-108
Preprint. Discussion started: 15 January 2026
© Author(s) 2026. CC BY 4.0 License.

(2024). Despite their limited surface area on the order of 0.1% of the global ocean, it has been estimated that they bury between 17 and 20 Tg yr^{-1} of organic carbon, equivalent to 11% of the annual marine organic carbon burial globally (Smith et al., 2015). These high rates have been attributed to very high area-normalised burial rates, about one hundred times as large as the global ocean average (Smith et al., 2015). Global organic carbon burial rates were reanalysed by Cui et al. (2016), yielding a wider range of 6.1 to 31 Tg yr^{-1} of organic carbon burial. In the above studies, burial rates were calculated assuming a burial efficiency of 80% in line with Berner (1980). However, burial efficiencies are in fact highly variable (e.g., Koziorowska et al., 2018: Tab. 5).

Conversely to burial rates, the total quantity of organic carbon stored in fjord sediments globally is largely unknown (Bianchi et al., 2020). However, a first national carbon inventory has been published for Scotland's fjords (Smeaton et al., 2017). According to this study, the mid-latitude fjords of Scotland hold 295.6 ± 52 Tg of organic carbon, of which 252.4 ± 62 Tg are stored in postglacial sediments and the remainder (43.2 ± 12 Tg) in glacial sediments. A subsequent study focussing on surficial (upper 10 cm) sediments showed that both sediment type and organic carbon content are spatially highly heterogeneous (Smeaton and Austin, 2019). In total, surface sediments of Scottish fjords were estimated to hold 4.2 ± 0.5 Tg of organic carbon, whilst Irish fjords and sea loughs store 2.1 ± 0.3 Tg of organic carbon.

Organic carbon in fjord sediments is either derived from local primary producers (autochthonous) such as phytoplankton and macroalgae or from external sources (allochthonous), such as terrestrial hinterlands, the coastal ocean or glaciers (Bianchi et al., 2020). This means that, while terrestrially sourced organic carbon is always allochthonous, marine organic carbon can be both autochthonous (when produced in the fjord) and allochthonous (when imported from the adjacent coastal ocean). Between 55 and 62% of the organic carbon buried in fjords globally and 76% in northwest Europe is terrestrially derived (Cui et al., 2016). Such average figures for large areas mask, however, the spatial variability of organic carbon sources, which is driven by the oceanographic setting (Faust and Knies, 2019).

The reactivity of sedimentary organic carbon is its susceptibility to biotic or abiotic decomposition (Cui et al., 2022; Graves et al., 2022) and is controlled by various factors such as organic matter composition, microbiology, thermodynamics, temperature effects and physical protection (Arndt et al., 2013). Based on globally distributed data from 25 fjords, Cui et al. (2022) show that the level of organo-mineral interaction governs the mean reactivity of organic carbon in contemporary fjord sediments, and also that organic carbon in fjord sediments is more thermally labile than that in global sediments. An estimated 61 ± 16% of the sedimentary organic carbon in fjord sediments are labile and easily degradable (Cui et al., 2022).

Even though global estimates as those presented above are important to assess the role of fjords in the carbon cycle, they are fraught with limitations such as small sample sizes that are not representative and generalisations that might not apply to specific subareas. An improved understanding of the spatial heterogeneity of fjord sediments and organic carbon can provide a foundation to reevaluate global estimates of organic carbon burial (Smeaton and Austin, 2019). The objective of this study therefore is to characterise the spatial heterogeneity of organic carbon stored in surficial (0 – 10 cm sediment depth) fjord sediments. Our study site is located north of the city of Stavanger, southwest Norway. We map substrate type and sedimentary environment, quantify organic carbon accumulation rates, stocks, provenance and reactivity. Based on our

https://doi.org/10.5194/egusphere-2026-108
Preprint. Discussion started: 15 January 2026
© Author(s) 2026. CC BY 4.0 License.

results and those from similar studies in northwest Europe, we provide evidence that global estimates are likely based on simplistic assumptions, which might have led to overestimations. Finally, we propose a framework for deriving more realistic global estimates of organic carbon burial in fjords.

2 Materials and methods

2.1 Study site

Our research is focussed on the marine area of Stavanger municipality in southwest Norway (Figure 1). The main connection of the fjord system to the open sea is via Boknafjorden in the northwest. The wider study site was mapped as part of the project Marine Base Maps for the Coastal Zone (https://www.ngu.no/geologisk-kartlegging/marine-grunnkart-kystnaer-havbunnskartlegging, last access: 15/12/2025) and has an area of approximately 500 km^2, with water depths ranging between 0 m and 714 m. Seabed substrate type and sedimentary environment were mapped within this area. Nested within the wider study site lies the core study site with an approximate area of 250 km^2 and water depths between 0 m and 583 m below sea level. Investigations on organic carbon in surface sediments were restricted to this area.

2.2 Mapping of substrate type and sedimentary environment

Maps of seabed substrate types (sediment grain size) and sedimentary environment are two of the main products of the Marine Base Map pilot project in Stavanger, and they are both full-coverage, scale 1:20 000 vector maps. Thematic vector maps are created through expert interpretation of multibeam echosounder (MBES) bathymetry and backscatter data indicating the seabed's topography and relative hardness. Interpretation is guided by ground-truthing sediment samples and visual observations of the seabed from towed camera or a remotely operated vehicle (ROV), and aided by 2D acoustic sub-bottom profiling lines, LIDAR and aerial photography data from adjacent land areas, and any relevant legacy data from previous surveys. Further details on seabed mapping through expert interpretation can be found in Elvenes et al. (2019) and Bøe et al. (2022).

In the pilot project, we planned locations for video observations using a stratified random sampling design. Close to 300 video lines were recorded in the 500 km^2 study area during fieldwork in 2020. 80 grab sample stations were placed by the field geologist in soft-sediment areas where ground-truthing was needed, and an additional 10 multi corer stations for geochemical analyses were distributed in basins across the study area (Knies et al., 2021a).

Out of NGU's 35 pre-defined classes of sediments used in seabed mapping (NGU, 2019a), we included 19 in the sediment grain size map of the wider study area. Most of these classes are also represented in the core study area of this project. In the map of sedimentary environment, we aim to describe whether conditions on the seabed allow for erosion or deposition of sandy or finer sediment. Five of NGU's standardised classes (NGU, 2019b) were found in Stavanger, all of which are also represented in the core study area. The Marine Base Maps for the Coastal Zone pilot project conducted in 2020 - 2022 was the first of NGU's coastal mapping projects to include sedimentary environment.

https://doi.org/10.5194/egusphere-2026-108
Preprint. Discussion started: 15 January 2026
© Author(s) 2026. CC BY 4.0 License.

2.3 Sampling design

We used a stratified random sampling design to avoid human bias and to facilitate modelling and spatial prediction based on 40 bulk samples of the uppermost 10 cm of the seabed sediment. Sampling within the core study site was limited to seabed areas where deposition from suspension, including limited local erosion of fine-grained sediments, was expected based on the mapped sedimentary environment (section 3.1). Of the 16 substrate classes found in these areas, six (human-made structures; gravel, cobbles and boulders; gravelly sand; sand; cobbles and boulders and cobbles/boulders covered by mud/sand) were excluded as they were deemed difficult to sample. However, these classes accounted for less than 1 km^2 of the seabed. Furthermore, the bathymetry data were classified into three depth intervals (shallow from 0 to 181 m, intermediate from 181 to 391 m, and deep from 391 to 583 m) using Jenk's natural breaks in ArcGIS 10.8.2. Strata were derived by combining the ten substrate classes with the three depth classes. Of the theoretically possible 30 strata, 24 did exist in the core study site. Before stations were randomly placed, we removed areas that were not accessible to sampling (aquaculture and military areas). Strata with an area of less than 1 km^2 were combined with suitable neighbouring strata. The stratified random placement of the stations was executed with the NOAA Sampling Design Tool for ArcGIS. The chosen allocation method was proportional, i.e., the number of stations per stratum was based on the relative area size of the strata. This led to 38 out of 40 stations being automatically allocated by the sampling tool. The two remaining stations were allocated to two strata, which had not automatically received a station.

Of the stations that fell into areas mapped as deposition from suspension, ten were selected to collect short cores that were dedicated to dating and the calculation of accumulation rates (Figure 2).

2.4 Field sampling and laboratory analysis

Fieldwork was conducted from 13th to 17th June 2023 onboard the 24 m research vessel 'Geologen'. Short sediment cores and grab samples were collected at the planned stations. The choice of sampling equipment depended on the substrate type at each station. Homogeneous, fine-grained sediments (mud and sandy mud) were sampled with a multi corer, which was equipped with four tubes of 60 cm length with a diameter of 6.3 cm. The tubes are closed at the top and bottom as the sample is taken, so that each core sample is collected with an undisturbed sediment surface. In coarser substrate types with a higher proportion of sand and gravel content, the samples were taken with a van Veen grab. Bulk samples of the upper 10 cm of sediment were taken at each station. When the multi corer was used, the upper 10 cm were cut off with a plastic spatula and frozen in plastic bags. When using a grab, four 10 cm long samples were taken with a syringe, collected in a plastic bag and frozen. At ten of the 40 stations, samples were also taken for dating (Figure 2). A sediment core from the multi corer was cut into 2 cm slices down to 20 cm sediment depth. The slices were packed separately in plastic bags and frozen after weighing. After fieldwork, all samples were sent to the laboratory at the Geological Survey of Norway (NGU). The samples were freeze-dried and further analysed. Dry bulk density (r_d) was calculated from the total water content of a sample using an

https://doi.org/10.5194/egusphere-2026-108
Preprint. Discussion started: 15 January 2026
© Author(s) 2026. CC BY 4.0 License.

empirical equation (Flemming and Delafontaine, 2000). Total organic carbon content (G) was measured using a LECO SC632 sulphur/carbon analyser.

Station-wise organic carbon stocks (OCS) were calculated using measurements on dry bulk density (r_d) and total organic carbon content (G) and the sediment thickness (d = 0.1 m):

$$OCS\ (kg\ m^2) = \frac{G\ (\%)}{100\%} \cdot 1000 \cdot \rho_d (g\ cm^{-3}) \cdot d(m) \quad (1)$$

The carbon reactivity index (CRI) is a measure to characterise the thermal reactivity of organic matter (Smeaton and Austin, 2022a). The CRI represents a continuum of reactivity with a value of 0 indicating that the organic matter is fully reactive and a value of 1 indicating that the organic matter is not reactive. In reality, these extremes will not be reached. The CRI was determined based on thermogravimetric analysis at the University of St. Andrews, Scotland. Milled samples of approximately 20 mg were placed into 70 ml aluminium oxide crucibles before being placed into a Mettler Toledo TGA2 and heated from 40 °C to 1000 °C at a ramp heating rate of 10 °C min^{-1} under a constant stream of N_2. Analytical accuracy of the TGA analysis was determined through the measurement of, Calcium Oxalate Monohydrate (COM) using the same instrument parameters as the samples. COM degrades at three distinct temperatures 150 °C, 500 °C and 750 °C (Hourlier, 2019). The COM (*n = 5*) thermograms on average deviate from the known thermal profile by 0.16 ± 0.04 °C and differences in mass loss between all standards by 1.23% ± 0.41%. The thermograms produced from these analyses were adjusted to a common temperature scale and clipped to the range 200 °C–650 °C to remove interference from absorbed water and non-organic material. The thermograms were normalised to the mass loss, to assure all thermograms were comparably scaled. Note that a high CRI value indicates a low fraction of labile organic matter and vice versa.

Stable carbon isotopes of the organic carbon fraction ($d^{13}C_{org}$) was undertaken at the University of St Andrews. Approximately 12 mg of milled sediment was placed into silver capsules. The samples then underwent acid fumigation (Harris et al., 2001) to remove carbonate ($CaCO_3$), post fumigation the samples were dried for 48 hr at 40°C and sealed prior to analysis. Stable isotope analysis was undertaken using an elemental analyser coupled to an isotope ratio mass spectrometer. Quality control was assured by repeat analysis of high organic carbon sediment standard (B2151) with reference values for C of 7.45% ± 0.14% and $\delta^{13}C$ of −28.85 ± 0.10‰. The reference standards (*n = 10*) deviated from their known values by: OC = 0.05%, $\delta^{13}C$ = 0.09‰. The isotope values are reported in standard delta notation relative to Vienna Peedee belemnite (VPDB).

Samples for dating were sent to the Gamma Dating Center Copenhagen at the University of Copenhagen, where the activity of the isotopes ^{210}Pb, ^{226}Ra and ^{137}Cs was analysed using gamma spectrometry. The measurements were carried out on a Canberra ultralow-background Ge-detector. ^{210}Pb was measured via its gamma-peak at 46.5 keV, ^{226}Ra via the granddaughter ^{214}Pb (peaks at 295 and 352 keV) and ^{137}Cs via its peak at 661 keV. Constant rate of supply modelling has been applied on the profile using a modified method (Andersen, 2017; Appleby, 2001), where the activity below the lower-

https://doi.org/10.5194/egusphere-2026-108
Preprint. Discussion started: 15 January 2026
© Author(s) 2026. CC BY 4.0 License.

most sample is calculated based on a regression of unsupported ^{210}Pb vs accumulated dry density. Based on the radiometric data, the age of the sediment at different depths and ultimately mass accumulation rates (MAR) could be determined for each analysed core sample. In addition to the ten cores collected in 2023, we also included data from two cores collected and analysed as part of the Marine Base Maps for the Coastal Zone project (Knies et al., 2021a). These were collected with the same type of multi corer.

Organic carbon accumulation rates ($OCAR_{10}$) were calculated from average mass accumulation rates ($\overline{MAR}$) and organic carbon content ($\bar{G}$) of the upper 10 cm of the analysed cores:

$$OCAR_{10}\ (g\ m^{-2}\ yr^{-1}) = 1000 \cdot \overline{MAR}(kg\ m^{-2} yr^{-1}) \cdot \frac{\bar{G}(\%)}{100\%} \quad (2)$$

2.5 Modelling and spatial prediction

The response variables organic carbon stock, carbon reactivity index and stable carbon isotopes were spatially predicted based on models derived from the 40 bulk samples. The number of stations (n = 12) was, however, not sufficient to model and spatially predict organic carbon accumulation rates.

The same predictor variables were used for all three response variables. These included acoustic data from multibeam surveys (bathymetry and backscatter strength), the Euclidean distance to the nearest shoreline, semi-quantitative substrate composition (mud, sand, gravel, cobbles/boulders and bedrock) derived from the mapped substrates, photosynthetically active radiation (400 – 700 nm wavelength) reaching the seabed, modelled salinity, temperature and current velocity at the seabed (mean, standard deviation, minimum and maximum) and the 90th percentile of the wave orbital velocity at the seabed (Table S1).

Modelling was carried out with Quantile Regression Forests (Meinshausen, 2006). Since the response data were collected as a probability sample (stratified random sample in this case), it was sufficient to estimate model performance with 10-fold cross validation without the need to account for spatial autocorrelation in the data (Meyer and Pebesma, 2022; Wadoux et al., 2021). The model performance was assessed with three metrics: the mean error (which measures bias), the root mean squared error (which measures accuracy) and the r-squared (which measures the explained variance). The set of predictor variables finally selected for prediction was determined through forward feature selection (Meyer et al., 2018). Based on the selected models, we spatially predicted the response variables and their area of applicability (Meyer and Pebesma, 2021). We also estimated the area of applicability (Meyer and Pebesma, 2021). Within the area of applicability, the combination of predictor variables is similar to what the model has been trained with. Outside the area of applicability, the predictions might extrapolate beyond the predictor variable space that has been captured by the model and results might thus be unreliable.

Finally, we quantified spatially explicit model uncertainty with the 90% prediction interval, PI90 (Heuvelink, 2014). The

https://doi.org/10.5194/egusphere-2026-108
Preprint. Discussion started: 15 January 2026
© Author(s) 2026. CC BY 4.0 License.

PI90 gives the range of values within which the true value is expected to occur nine times out of ten, with a one in 20 probability for each of the two tails (Arrouays et al., 2014). It is defined as

$$PI90 = q_{0.95} - q_{0.05} \quad (3)$$

with $q_{0.95}$ and $q_{0.05}$ being the 0.95 and 0.05 quantiles of the distribution, respectively.

Finally, we corrected the predicted organic carbon stocks for the fraction of coarse substrates. We assumed that cobbles, boulders and bedrock do not contain organic carbon. The predicted stocks (OCS_{pred}) were hence corrected (OCS_{corr}) based on the coarse fraction (CSF) according to:

$$OCS_{corr} = OCS_{pred} \cdot (1 - CSF) \quad (4)$$

The reservoir size and its uncertainty were calculated by summing corrected organic carbon stocks and associated uncertainties over all pixels of the resulting raster layers and multiplying with the area of one pixel (2,500 m^2).

2.6 Regionalisation

An unsupervised classification was carried out to provide a regionalisation of the study site. The regionalisation was based on the spatially predicted variables organic carbon stocks, carbon reactivity index and stable carbon isotopes. A k-means clustering was conducted utilising the algorithm of Hartigan and Wong (1979). Prior to clustering, the input variables were normalised. The selection of the number of clusters to be requested was aided by an elbow plot. Box plots of the clusters for the three variables were created based on a subsample (n = 10,000) to visualise the properties of the clusters.

2.7 National scale estimates

To put our results from the local study in a wider context, we analysed maps of seabed substrate and sedimentary environment from other coastal areas derived by the Geological Survey of Norway over the last 20 years or so. Initially, these GIS vector maps were clipped to the area covered by the Norwegian fjord catalogue (https://data.norge.no/en/datasets/e34a3447-dc8b-4661-9361-ec72da8109af/fjordkatalogen). They were subsequently dissolved as multipart features by substrate type and sedimentary environment, respectively. Finally, the geodesic area was calculated with the Add Geometry Attributes tool. The analysis was performed in ArcGIS Desktop 10.8.2.

We also compiled data from other fjords in mainland Norway and calculated organic carbon accumulation rates for the upper 10 cm ($OCAR_{10}$) following eq. 2.

https://doi.org/10.5194/egusphere-2026-108
Preprint. Discussion started: 15 January 2026
© Author(s) 2026. CC BY 4.0 License.

3 Results

3.1 Substrate type and sedimentary environment

Full-coverage, high-quality MBES data of 1 to 2 m resolution combined with a high number of seabed observations allowed for detailed mapping of substrate type in the study area (Figure 3). Backscatter data were especially useful in delineating areas of soft sediment (sandy or muddy substrate types reflecting less of the acoustic echosounder signal than what coarser seabed does), while bathymetry data revealed landforms like moraine ridges, talus cones or bedrock outcrops associated with harder substrates. In shallow areas the data could even show individual boulders. Keeping to a map scale of 1:20 000 requires some generalisation, as individual map elements cannot be too small to distinguish at the intended scale. Much of the Stavanger seabed is also of a heterogeneous nature, with both sand/mud and rocks/boulders present in the same area. This heterogeneity is expressed in map form by the use of mixed classes such as "Sand, gravel, cobbles and boulders" or "Mud and sand with gravel, cobbles and boulders".

As shown in Table 1, around a third of the seabed in the study area is defined as "Thin or discontinuous sediment cover on bedrock". Note that the classification does not distinguish between different types of sediment cover, and as such may include both fine-grained and very coarse material covering bedrock in various thicknesses. The seabed type is also found at all depths (Figure 3). Mud and sandy mud cover 12.0% and 13.6% of the seabed, respectively, dominating deeper areas and some isolated basins. Another 11.9% of the seabed is defined as the heterogeneous substrate type "Sand, gravel, cobbles and boulders", found predominantly in areas shallower than 200 m. Other substrate types cover less than 10% of the seabed, with only "Gravelly sandy mud" and "Mud and sand with gravel, cobbles and boulders" exceeding 5%. 48.5 km^2 of the area are characterised by deposition from suspension, and 78.4 km^2 by deposition from suspension with local erosion of fine-grained sediments. The remainder (126.5 km^2) either shows signs of erosion or deposition of mainly sand from bottom currents. This means that half of the area is depositional in character (Figure 4).

At the national scale, the inshore areas covered by the fjord catalogue amount to 89,368.4 km^2. Of this, 13,768 km^2 (15.4%) have so far been mapped with regard to substrate types and 2,604.9 km^2 (2.9%) with regard to the sedimentary environment. Fine-grained sediments (mainly mud, sandy mud and muddy sand but including clay, organic mud, mud with sediment blocks, silt, sandy silt and silty sand (NGU, 2019a)) cover 33.1% of the mapped area. Environments conducive to sediment deposition (deposition from suspension and deposition from suspension, local erosion of fine-grained sediments) cover 35.5% of the mapped seabed.

3.2 Data exploration

The three response variables organic carbon stock, stable carbon isotope values and the carbon reactivity index are plotted in a generalised pairs plot together with the water depth at the sampling locations (Figure 5). Organic carbon stocks display a distribution with a dominant peak at approximately 0.75 kg m^{-2}. Stable carbon isotope values exhibit a bimodal distribution with peaks at approximately -22.5‰ and -26‰, indicating marine and terrestrial sources, respectively. The distribution of

https://doi.org/10.5194/egusphere-2026-108
Preprint. Discussion started: 15 January 2026
© Author(s) 2026. CC BY 4.0 License.

CRI values is also bimodal but has a dominant peak at 0.725 and a secondary peak at 0.625. All three response variables show strong and statistically significant ($p < 0.001$, $n = 40$) correlations with each other. Organic carbon stocks are negatively correlated with stable carbon isotope and CRI values, while the latter two exhibit a positive correlation. The response variables are also correlated with water depth, albeit less strongly.

3.3 Organic carbon accumulation rates

To obtain reliable results, sediment mixing due to bioturbation or other processes has to be negligible; otherwise, the accumulation rates will be overestimated. There were two cores with significant mixing (marked by ** in Figure 6) and two cores with possible mixing (marked by * in Figure 6), while the rest of the cores showed no signs of sediment mixing based on examination of the ^{210}Pb profiles. The calculated accumulation rates in the cores with sediment mixing are therefore probably overestimated. At the same time, the values are low compared to data from cores without mixing. To obtain a more representative overview of the accumulation rates, we therefore do not exclude the cores with signs of sediment mixing but note that these rates might be too high.

Estimated organic carbon accumulation rates varied from 18.7 g m^{-2} yr^{-1} to 82.6 g m^{-2} yr^{-1} (Figure 6), with a mean value of 44.6 g m^{-2} yr^{-1}. There are no clear spatial patterns apparent and organic carbon accumulation rates can change over short distances, e.g. in Talgjefjorden between Rennesøy and Finnøy.

At the national level, $OCAR_{10}$ could be calculated for 28 cores from five regions. Apart from Stavanger (Diesing et al., 2024b; Knies et al., 2021a), these were Sunnhordland (Knies et al., 2024), Sunnmøre (Knies et al., 2021b), Sør-Troms (Lepland et al., 2012) and Troms (Knies et al., 2022). The data from Stavanger was supplemented with four values from Høgsfjorden and Lysefjorden (Duffield et al., 2017), immediately to the east of our study site (Figure 1). The data are compiled in Table S2. The median $OCAR_{10}$ of these 28 records is 40.5 g C m^{-2} yr^{-1} (Table 2).

3.4 Organic carbon stocks

Seven predictor variables were selected for the final organic carbon stock model (gravel content, maximum bottom salinity, mean bottom temperature, maximum bottom current velocity, 90% percentile of the wave orbital velocity at the seabed, mean bottom salinity and minimum bottom temperature). The model had a mean error (ME) of 0.012 kg m^{-2}, a root mean squared error (RMSE) of 0.174 kg m^{-2}, an explained variance (R^2) of 59.2% and an area of applicability equal to 98% of the total area.

The corrected organic carbon stocks varied between 0.1 kg m^{-2} and 1.37 kg m^{-2} (Figure 7), while the PI90 ranged from 0.14 kg m^{-2} to 1.15 kg m^{-2} (Figure S1). Organic carbon stocks were highest in the central part of Mastrafjorden between Rennesøy and Mosterøy and some smaller areas in the eastern part of the study site. Stocks are lowest in scattered areas mapped as thin or discontinuous sediment cover on bedrock (Figure 3). In total, 83.2 ± 55.7 Gg of organic carbon are stored in the surface sediments of the mapped area.

https://doi.org/10.5194/egusphere-2026-108
Preprint. Discussion started: 15 January 2026
© Author(s) 2026. CC BY 4.0 License.

3.5 Sources of organic carbon

Three predictor variables were selected for the final $d^{13}C$ model (bathymetry, maximum bottom current velocity and the 90% percentile of the wave orbital velocity at the seabed). The model had an ME of 0.039‰, an RMSE of 0.822‰, an R^2 of 82.7% and an area of applicability (AOA) equal to 90% of the total area.

Predicted $d^{13}C$-values varied between -27.33‰ and -21.78‰ (Figure 8), while the PI90 ranged from 1.47‰ to 6.21‰ (Figure S2). The d13C-values are highest in Boknafjorden in the west of the study site and in Talgjefjorden between Rennesøy and Finnøy.

3.6 Reactivity of organic carbon

Four predictor variables were selected for the final CRI model (bedrock, standard deviation of bottom temperature, 90% percentile of the wave orbital velocity at the seabed and the maximum bottom current velocity). The model had an ME of 0.001, an RMSE of 0.027, an R^2 of 80.3% and an area of applicability equal to 87% of the total area.

Predicted CRI values varied between 0.59 and 0.78 (Figure 9), while the PI90 ranged from 0.04 to 0.21 (Figure S3). The spatial patterns resemble those of the stable carbon isotope values (Figure 8). This might be expected since $d^{13}C$ and CRI exhibit a strong positive correlation (Figure 5).

3.7 Regionalisation

Based on an elbow plot, a four-cluster solution was selected. The cluster numbers were ordered in a way that the mean $d^{13}C$-values per cluster decreased (Figure 10). Cluster 1 (dark blue) is characterised by intermediate organic carbon stocks, high $d^{13}C$-values and high CRI-values and is located in the central (deeper) parts of Boknafjorden, Talgjefjorden and Finnøyfjorden. Cluster 2 (light blue) exhibits low organic carbon stocks, a high variability in $d^{13}C$-values and relatively high CRI-values. The cluster has a high association with seabed areas dominated by a thin or discontinuous sediment cover on bedrock and other coarse substrates. Cluster 3 (light green) has intermediate organic carbon stocks, relatively low $d^{13}C$-values and intermediate to low CRI-values. The cluster is mainly found in Finnøyfjorden, Fognafjorden and Gardssundfjorden. Cluster 4 (dark green) shows the highest organic carbon stocks, the lowest $d^{13}C$-values and the lowest CRI-values. This cluster is most prominent in Mastrafjorden and restricted areas in the northeast of the study site.

4 Discussion

4.1 Environmental variability

We provide evidence for strong variability along various environmental gradients (substrate type, sedimentary environment, organic carbon accumulation rates, stocks reactivity and source). Substrate types vary from mud (clay and silt) to cobbles and boulders, and a third of the seabed is bedrock covered by a thin and discontinuous layer of sediment. Fine-grained

https://doi.org/10.5194/egusphere-2026-108
Preprint. Discussion started: 15 January 2026
© Author(s) 2026. CC BY 4.0 License.

sediments (mud, sandy mud and muddy sand) collectively cover just over 30% of the seafloor in Stavanger, similar to the percentage at the national scale (33%). Comparable fractions are found to cover the seabed in the fjords of Scotland and Ireland (Smeaton and Austin, 2019) Half of the mapped area in Stavanger is characterised by transport and erosion, while deposition of fine-grained sediment is restricted to the other half. At the national scale, depositional areas account for 35% of the mapped seabed in mainland Norway.

Calculated organic carbon accumulation rates vary between 19 and 83 g C m^{-2} yr^{-1} in Stavanger. In the nearby fjords to the east of our study site, values of 13 – 171 g C m^{-2} yr^{-1} were reported for Høgsfjorden and Lysefjorden, with the highest rates recorded at the head of Lysefjorden closest to the Lyseåna river (Duffield et al., 2017). Comparable rates of 43 – 133 g C m^{-2} yr^{-1} were also found in Raunefjorden (Włodarska-Kowalczuk et al., 2019). The mean value of 44.6 g m^{-2} yr^{-1} for Stavanger falls within the range of mean values reported from fjord systems in northwest Europe: 28.0 g C m^{-2} yr^{-1} in east Iceland (Watts et al., 2025), 38.0 g C m^{-2} yr^{-1} at the west coast of Sweden (Watts et al., 2024) and 57.1 g C m^{-2} yr^{-1} in Scotland (Smeaton et al., 2021).

Corrected organic carbon stocks range from 0.1 to 1.37 kg m^{-2} in Stavanger, indicating considerable variability. However, the variability is lower than in fjords of Scotland and Ireland, where especially muddy sediments have stocks of 3 kg m^{-2} and more (Smeaton and Austin, 2019). Presumably, this difference in variability is linked to the different size of the areas. It might be assumed that on a national scale the variability in stock sizes in Norway is larger than in Stavanger.

Measured CRI values vary between 0.56 and 0.81 (i.e., labile organic matter fraction of 19% – 44%) in Stavanger. This falls within the range of values of 0.45 – 0.9 in inshore (fjords and estuaries) surface sediments outside hypoxic upper fjord basins in Scotland (Smeaton and Austin, 2022a). Organic matter sampled in these hypoxic basins has an even higher labile fraction of up to 69% (Smeaton and Austin, 2022a).

Measured $d^{13}C$-values range from -27.44‰ to -21.23‰, with a bimodal distribution showing peaks at -26‰ and -22.5‰ (Figure 5). The minima and maxima are close to reported terrestrial and marine end members in Norway and Scotland of -26.1‰ to -28.6‰ and -18.7‰ to -20.6‰, respectively (Faust and Knies, 2019; Knies and Martinez, 2009; Smeaton et al., 2021; Smeaton and Austin, 2017; Winkelmann and Knies, 2005). Using a two-end-member mixing model (Thornton and McManus, 1994) and assuming that the terrestrial (-28.56‰) and marine (-18.99‰) end member values determined by Smeaton and Austin (2022b) are applicable to our study site, indicates that the terrestrial fraction of organic carbon might range between 23% and 88%. These results demonstrate a strong variability of the sources of organic carbon over a comparatively small area. A high variability of sources was also found in fjords of the Swedish west coast (-27‰ to -20‰, Placitu et al., 2024) and in the fjords of Scotland (-29.7‰ to -19.5‰, Smeaton and Austin, 2022b), while in other regions $d^{13}C$-values are more constrained, e.g., Reyðarfjörður and Berufjörður in Iceland (-23.2‰ to -21.8‰, Watts et al., 2025) and Ofotfjorden, Tysfjorden and Vestfjorden in northern Norway (-23.8‰ to -20.9‰, Faust and Knies, 2019).

In summary, we observe high variability especially regarding substrate types and the depositional environment, organic carbon accumulation rates and the source of organic carbon.

https://doi.org/10.5194/egusphere-2026-108
Preprint. Discussion started: 15 January 2026
© Author(s) 2026. CC BY 4.0 License.

4.2 Spatial heterogeneity

Our results point towards strong spatial heterogeneity in Stavanger. Organic carbon accumulation rates can vary over short distances (a few kilometres), as exemplified by three cores taken in Talgjefjorden (Figure 6). These cores encapsulate the full variability of calculated organic carbon accumulation rates (19 and 83 g C m^{-2} yr^{-1}) in Stavanger. Presumably, the highest of the three rates is due to the coring location close to the centre of the basin, while the other two cores exhibiting lower rates have marginal positions in the basin. As the central coring location was deliberately chosen for the purpose of investigating the historical development of contamination (Knies et al., 2021a) while the other two locations were chosen randomly as described in section 2.3, these observed differences also highlight the influence of the sampling design. Using non-randomly selected coring locations will most likely bias the data towards high organic carbon accumulation rates.

The central (deeper) parts of Boknafjorden, Talgjefjorden and Finnøyfjorden are characterised by high $d^{13}C$-values (cluster mean: -22.5‰) close to reported marine end member values of -18.7‰ to -20.6‰ in Norway and Scotland (Faust and Knies, 2019; Knies and Martinez, 2009; Smeaton et al., 2021; Smeaton and Austin, 2017; Winkelmann and Knies, 2005) and CRI values (cluster mean: 0.73) typical of coastal and offshore zones in Scotland (Smeaton and Austin, 2022a) (Cluster 1 in Figure 10). Boknafjorden is directly connected to the northern North Sea and marine water can enter the fjords in Stavanger via Boknafjorden, Talgjefjorden and Finnøyfjorden as evidenced by our data.

Conversely, shallow fjords like Mastrafjorden and the shallow areas between Finnøyfjorden and Strandafjorden in the northeast of the core study site are characterised by low $d^{13}C$-values (cluster mean: -26.1‰) close to terrestrial end member values of -26.1‰ to -28.6‰ (Faust and Knies, 2019; Knies and Martinez, 2009; Smeaton et al., 2021; Smeaton and Austin, 2017; Winkelmann and Knies, 2005) indicating strong terrestrial influence (Cluster 4 in Figure 10). CRI values (cluster mean: 0.62) are similar to those of inshore (fjords and estuaries) zones (Smeaton and Austin, 2022a). Marine influence is likely dictated by bathymetry. Remarkably, the strikingly different Clusters 1 and 4 are found in close proximity to each other, e.g. the distance between Talgjefjorden and Mastrafjorden is approximately 5 km. The two clusters are spatially separated by the two transitional Clusters 2 and 3.

In summary, fjords in Stavanger are spatially heterogeneous, echoing results from Scotland and Ireland (Smeaton and Austin, 2019).

4.3 Upscaling to higher levels

The previous sections have demonstrated that fjords in northwest Europe are systems with a high spatial heterogeneity and variability in parameters relating to organic carbon in sediments. In the following, we review upscaling practices and to what extent they are likely to capture the described heterogeneity and variability.

Apart from Scottish and Irish fjords (Smeaton and Austin, 2019), there have been no attempts published in the peer-reviewed literature to upscale organic carbon stocks to the national level or higher. The authors used a tiered approach consisting of interpolated point data (tier 1) and acoustic backscatter data classified via clustering and ground-truthed with sediment type

https://doi.org/10.5194/egusphere-2026-108
Preprint. Discussion started: 15 January 2026
© Author(s) 2026. CC BY 4.0 License.

data (tier 2). Both tiers were combined to derive composite sediment type maps (tier 3). Statistics on organic carbon and dry bulk density from collected samples were then calculated for the different sediment types and these were used to upscale to the national level. It can be expected that such an approach yields realistic estimates when organic carbon and dry bulk density have been sampled in a representative way. However, this does usually require collecting new samples with an appropriate sampling design, as legacy data are likely biased. In addition, a prerequisite for this approach is that the seabed sediment types have been mapped in the area of interest.

The quantification of the reactivity of organic matter and carbon has recently become a routine analytical process with the introduction of methods based on thermogravimetric, ramped oxidation and ramped pyrolysis analysis (Cui et al., 2022; Hemingway et al., 2017; Rosenheim et al., 2013; Smeaton and Austin, 2022a). Spatial coverage is however still sparse, e.g., CRI measurements on seabed sediments are available from the United Kingdom and Norway only (Diesing et al., 2025; Smeaton and Austin, 2022a). Cui et al. (2022) estimated the reactivity of sedimentary organic carbon in global fjords based on 33 surface sediment samples from 25 fjords in Greenland (2), Svalbard (4), northern Europe (3), southeast Alaska (6), eastern Canada (1), western Canada (1), Patagonia (4), New Zealand (3) and Antarctica (1). They investigated the spatial heterogeneity along three fjord proximal-to-distal transects with contrasting sources of organic carbon (marine, terrestrial and petrogenic). They concluded that despite the spatial variability of organic carbon sources and their degradation states, the thermal reactivity of samples from the middle reaches was constrained well within the range of fjord distal and proximal sediments and most representative of the mean activation energy of sedimentary organic carbon in each fjord. Based on this finding the investigation was extended to the middle reaches of 22 large fjords from around the world. Even though the geographic spread does capture the global distribution of fjords, it would appear questionable whether the focus on middle reaches and the low number of samples per region and overall can yield an unbiased sample given the expected high spatial variability of fjords with respect to depositional environment and substrate type.

The fraction of terrestrial organic carbon in global fjord sediments was estimated by Cui et al. (2016) based on data from more than 300 fjord samples using end member mixing models. They found that the fractions of terrestrial organic carbon ranged between 42% in Chile and 76% in northwest Europe. The global average was 55% ± 14%, when excluding Greenland due to only one available sample; otherwise, it was 62%. These regional and global averages do however mask the strong variability found between and within fjord systems. Organic carbon is terrestrially dominated in fjord settings with either low marine and freshwater inflow or low marine and high freshwater inflow (Faust and Knies, 2019). Fjord systems with high marine and low freshwater inflow are marine dominated, while fjords with high marine and freshwater inflow show a substantial gradient from marine to terrestrial sources. Stavanger, with a range of $d^{13}C$-values reaching close to both end members, is an example of the latter case, as is Trondheimsfjorden in central Norway (Faust et al., 2014). Ofotfjorden, Tysfjorden and Vestfjorden in northern Norway are marine dominated (Faust and Knies, 2019), while Norwegian fjords (Kyllaren, Framvaren and Drammensfjorden) included in Cui et al. (2016) are terrestrially dominated. The average of 76% terrestrial organic carbon in northwest Europe (Cui et al., 2016), which is essentially based on the latter fjords from southern and western Norway, is therefore not representative for Norway as a whole nor northwest Europe either.

https://doi.org/10.5194/egusphere-2026-108
Preprint. Discussion started: 15 January 2026
© Author(s) 2026. CC BY 4.0 License.

Smith et al. (2015) used two methods to estimate global organic carbon burial in fjord sediments. In their method 1, they multiplied the sediment load (815 Tg yr^{-1}) delivered to fjords (Dürr et al., 2011) with an average organic carbon content (2.6 weight-%) derived from a data compilation containing 573 surface sediment samples, representing nearly all global fjord systems. In their method 2, they multiplied the global fjord area (455,000 km^2) according to Dürr et al. (2011) with an average organic carbon accumulation rate (54 g C m^{-2} yr^{-1}) derived from 124 sediment cores from the literature. In both methods, they assumed burial efficiencies of 80% in line with Berner (1982).

Cui et al. (2016) updated these estimates by using organic carbon content in surface sediments weighted by mass accumulation rates (method 1) and an updated collation of organic carbon accumulation rates (method 2). They attributed the large discrepancy in their estimates (6.1 and 31 Tg yr^{-1}) to either an underestimation of the global sediment load or an overestimation of the global fjord surface area and thought the former was more likely. The recently published fjord area of c. 260,000 km^2 (Laruelle et al., 2024), which is 58% of the previous estimate (Dürr et al., 2011), might point to the latter. Overall, these contradictions point to a poorly constrained global fjord area, potentially because current definitions of what constitutes a fjord are too vague to allow an exact delineation. In addition, neither Dürr et al. (2011) nor Laruelle et al. (2024) provide maps of the extent of fjords.

An implicit assumption of the studies by Smith et al. (2015) and Cui et al. (2016) is that the whole fjord area is accumulating sediments. This is obviously not the case. In Stavanger, the fraction of the area where deposition of fine-grained sediment occurs amounts to 50%, while on the national scale the current estimate is just over a third (section 3.1). In Scotland and Ireland, 26 – 33% of the fjord area are dominated by muddy sediments (Smeaton and Austin, 2019). Taken together, these results might indicate that only a quarter to one half of the fjord area in northwest Europe might be depositional in character.

Another implicit assumption of the studies by Smith et al. (2015) and Cui et al. (2016) is that the data compiled from various publications are representative of fjord environments. However, most geochemical studies deliberately select coring sites in the deepest and quietest basins of fjords to increase the chances of retrieving a core free from bioturbation and sediment mixing. In fact, standard dating techniques, such as the constant rate of supply methodology (Appleby, 2001) require undisturbed core sediments to yield reliable results. It is therefore questionable whether the data compilations used for global upscaling of organic carbon accumulation rates are representative. It is probably more likely that they are biased towards high values, as demonstrated by the results of threes cores in Talgjefjorden discussed in chapter 4.2.

Finally, previous studies (Cui et al., 2016; Smith et al., 2015) used a global burial efficiency of 80% to convert rates of organic carbon accumulation to burial. Current evidence suggests, however, that burial efficiencies in fjord sediments are highly variable (Koziorowska et al., 2018).

In summary, it would appear that current global estimates of organic carbon accumulation in fjord sediments are not well constrained and most likely too high, given the bias towards high values in terms of area and organic carbon accumulation rates as outlined above. In the following section, we make suggestions how a more realistic upscaling of local results to higher levels might be achieved.

https://doi.org/10.5194/egusphere-2026-108
Preprint. Discussion started: 15 January 2026
© Author(s) 2026. CC BY 4.0 License.

4.4 Requirements for realistic upscaling

We propose the following steps to achieve more realistic results when upscaling from local studies to a higher level, be it regional, national, continental or global. These considerations apply to variables that relate to the surface area of the seabed, i.e. organic carbon accumulation rates and stocks.

Step 1. Derive a realistic estimate of the total fjord area. This should be relatively straight forward at the local to regional level. However, the higher the level becomes the more difficult it is to derive realistic estimates. As shown before, the global fjord area is poorly constrained and there are no spatial products available. Higher level fjord maps might be derived through a GIS analysis utilising suitable data such as coastlines, bathymetry etc. Alternatively, fjord maps might be derived from remote sensing data analysed with machine learning algorithms similar to tidal flats (Murray et al., 2019).

Step 2. Estimate the fraction of seabed where fine-grained sediment accumulates. In Norway, these areas are mapped by experts as described in section 2.2. However, this process is time-consuming and requires suitable datasets (multibeam bathymetry, backscatter strength, sub-bottom, and ground-truthing data) to be collected in the first instance. As a proxy, sediment accumulation basins could be derived from existing seabed sediment maps by reclassifying mud-rich seabed types (Elvenes et al., 2019). However, these are likely to underestimate the true area where deposition of fine-grained sediments occurs. Alternatively, numerical models simulating sediment dynamics should be capable of identifying erosional and depositional areas. Due to the computational requirements of such models, they likely perform best on a local to regional level. Another option might be employing terrain variables derived from bathymetric data of sufficient resolution. Terrain variables such as roughness and bathymetric position index might be indicative of areas where sediment accumulates.

Step 3. Draw a representative sample of organic carbon accumulation rates or stocks. Ideally, a probability sample (such as a random or stratified random sample) should be drawn from the area for which an analysis is performed. However, such an approach is most likely restricted to local studies, as it involves the collection of a sufficient amount of new data. At higher levels, there is a need to include existing data from previous studies, but these data might be biased as discussed above. This could be visually checked by plotting spatial distance distributions (Meyer and Pebesma, 2022). Note that in the case of organic carbon stocks, the sediments in erosional and non-depositional areas (typically sands and gravels) will to some extent contain organic carbon (Smeaton and Austin, 2019).

Step 4. Account for uncertainty. Rather than just providing an estimate based on mean values, we suggest considering the variability of the data. This could be achieved by providing low and high estimates based on certain percentiles of the data distribution, e.g., P5 and P95 (Diesing et al., 2017; Donato et al., 2011).

To demonstrate the above, we use data from mainland Norway to give a tentative estimate of annual organic carbon accumulation in Norwegian fjord sediments. We also discuss the current limitations and suggest improvements.

The total area of the Norwegian fjord catalogue amounts to A_f = 89,368.4 km^2. The fraction of the seabed where deposition of fine-grained sediment dominates (f_{dep}) might be estimated to 25% (low), 33% (intermediate) and 50% (high estimate), based on the results from this study and Smeaton and Austin (2019). We use the data in Table 2 for values of organic carbon

https://doi.org/10.5194/egusphere-2026-108
Preprint. Discussion started: 15 January 2026
© Author(s) 2026. CC BY 4.0 License.

accumulation rates. In particular, we use the P5 for the low, the median for the intermediate and the P95 for the high estimate. We then calculate the annual organic carbon accumulation (OCA) for low, intermediate and high estimates by

$$OCA = A_f \cdot f_{dep} \cdot OCAR_{10}. \quad (5)$$

This yields 1.19 (0.41 – 3.68) Tg yr^{-1} of organic carbon accumulating in surface sediments of fjords in mainland Norway. Given a lack of data on burial efficiencies and inconsistencies in their definition (Bradley et al., 2022), we refrain from calculating organic carbon burial.

There are currently several limitations to these estimates. The total area (A_f) covered by the fjord catalogue includes sea areas which would not qualify as fjords in a strict geomorphological sense. The seaward limit of the fjord catalogue is the baseline relative to which maritime zones are defined, rather than a sill that separates a fjord from the open sea. The actual fjord area of mainland Norway is hence lower. However, from a practical point of view the baseline is a suitable seaward boundary as it is also the landward limit for which organic carbon stocks and accumulation rates have been derived in offshore areas (Diesing et al., 2024a). Using the baseline as the seaward limit of coastal and inshore areas ensures that there is no gap between coastal and offshore mapping.

The fraction of seabed characterised by deposition of fine-grained sediments (f_{dep}) is based on 3% of the total area where the sedimentary environment has been mapped in Norway. This estimate is therefore currently tentative, and we use three different values to account for uncertainty in the estimate. Inshore and coastal mapping in Norway is, however, ongoing and the fraction of mapped seabed will increase over time, yielding improved estimates.

So far, we have collated data on organic carbon accumulation rates ($OCAR_{10}$) from five regions, 19 fjords and 28 coring stations. Again, the estimates are tentative and we use the 5th and 95th percentiles of the data distribution to account for uncertainty, similar to Donato et al. (2011) and Diesing et al. (2017). The true organic carbon accumulation rate is likely to lie between the low (0.41 Tg C yr^{-1}) and the high estimate (3.68 Tg C yr^{-1}). As for the fraction of seabed characterised by deposition of fine-grained sediments, it can be expected that more data will be collected over the coming years, and the estimates will improve.

It should also be noted that the 28 cores used for this analysis were all retrieved from areas characterised by deposition from suspension. Collecting dateable cores from areas that are dominated by deposition from suspension but also show local erosion of fine-grained sediments is a challenging task. This is highlighted by the fact that those four cores located close to the boundary between the two areas show signs of sediment mixing (Figure 6). Improved dating techniques might be necessary to obtain realistic organic carbon accumulation rates from such transitional sedimentary environments.

https://doi.org/10.5194/egusphere-2026-108
Preprint. Discussion started: 15 January 2026
© Author(s) 2026. CC BY 4.0 License.

5 Conclusions

Based on detailed seabed mapping in fjords around Stavanger (Norway), we show that substrate types are highly variable and encompass the whole grain-size spectrum from mud to boulders. Areas where fine-grained sediments accumulate amount to 50% of the total mapped area. In these depositional areas, organic carbon accumulation rates and stocks vary considerably, as does the fraction of labile organic matter and the sources of organic carbon (marine vs terrestrial). This pronounced environmental variability, and spatial heterogeneity calls into question upscaling approaches that rely on implicit assumptions about the homogeneity of sediment type and depositional character and the representativeness of 'global' data compilations on organic carbon accumulation rates, reactivity and sources that are unlikely to hold. We conclude with suggestions of how upscaling from local to higher levels could be improved.

Code availability

All original code has been deposited at https://github.com/diesing-ngu/Stavanger_organic_carbon.

Data availability

Input data to spatially predict organic carbon stocks, the carbon reactivity index and $\delta^{13}C$ have been deposited at https://zenodo.org/records/18172827 (Diesing and Smeaton, 2026).

Supplement link

Supplement.docx

Author contributions

Conceptualization, MD, RB; Data curation, MD; Funding acquisition, RB; Investigation, MD, SE, CS; Methodology, MD, RB; Project administration, RB, MD; Resources, RB; Software, MD; Validation, MD; Visualization; MD; Writing (original draft preparation), MD, SE, CS; Writing (review and editing), MD, RB, SE, JK, CS

Competing interests

The authors declare that they have no conflict of interest.

https://doi.org/10.5194/egusphere-2026-108
Preprint. Discussion started: 15 January 2026
© Author(s) 2026. CC BY 4.0 License.

Acknowledgements

The authors would like to thank the captain and crew of R/V 'Geologen' for invaluable assistance during fieldwork.

Financial support

This work was financially supported by Stavanger municipality.

References

Andersen, T. J.: Some Practical Considerations Regarding the Application of 210Pb and 137Cs Dating to Estuarine Sediments, in: Applications of Paleoenvironmental Techniques in Estuarine Studies, edited by: Weckström Kaarina and Saunders, K. M. and G. P. A. and S. C. G., Springer Netherlands, Dordrecht, 121–140, https://doi.org/10.1007/978-94-024-0990-1_6, 2017.

Appleby, P. G.: Chronostratigraphic Techniques in Recent Sediments, in: Tracking Environmental Change Using Lake Sediments: Basin Analysis, Coring, and Chronological Techniques, edited by: Last William M. and Smol, J. P., Springer Netherlands, Dordrecht, 171–203, https://doi.org/10.1007/0-306-47669-X_9, 2001.

Arndt, S., Jørgensen, B. B., LaRowe, D. E., Middelburg, J. J., Pancost, R. D., and Regnier, P.: Quantifying the degradation of organic matter in marine sediments: A review and synthesis, Earth Sci Rev, 123, 53–86, https://doi.org/10.1016/j.earscirev.2013.02.008, 2013.

Arrouays, D., Grundy, M. G., Hartemink, A. E., Hempel, J. W., Heuvelink, G. B. M., Hong, S. Y., Lagacherie, P., Lelyk, G., McBratney, A. B., McKenzie, N. J., d.L. Mendonca-Santos, M., Minasny, B., Montanarella, L., Odeh, I. O. A., Sanchez, P. A., Thompson, J. A., and Zhang, G.-L.: Chapter Three - GlobalSoilMap: Toward a Fine-Resolution Global Grid of Soil Properties, vol. 125, edited by: Sparks, D. L., Academic Press, 93–134, https://doi.org/10.1016/B978-0-12-800137-0.00003-0, 2014.

Berner, R. A.: Early diagenesis: A theoretical approach, Princeton University Press, 256 pp., 1980.

Berner, R. A.: Burial of organic carbon and pyrite sulfur in the modern ocean: Its geochemical and environmental significance, Am J Sci, 282, 451–473, https://doi.org/10.2475/ajs.282.4.451, 1982.

Bianchi, T. S., Arndt, S., Austin, W. E. N., Benn, D. I., Bertrand, S., Cui, X., Faust, J. C., Koziorowska-Makuch, K., Moy, C. M., Savage, C., Smeaton, C., Smith, R. W., and Syvitski, J.: Fjords as Aquatic Critical Zones (ACZs), Earth Sci Rev, 203, 103145, https://doi.org/https://doi.org/10.1016/j.earscirev.2020.103145, 2020.

Bøe, R., Bjarnadóttir, L. R., Elvenes, S., Dolan, M., Bellec, V., Thorsnes, T., Lepland, A., and Longva, O.: Revealing the secrets of Norway's seafloor - geological mapping within the MAREANO programme and in coastal areas, Geological Society, London, Special Publications, 505, 57–69, https://doi.org/10.1144/SP505-2019-82, 2022.

https://doi.org/10.5194/egusphere-2026-108
Preprint. Discussion started: 15 January 2026
© Author(s) 2026. CC BY 4.0 License.

Bradley, J. A., Hülse, D., LaRowe, D. E., and Arndt, S.: Transfer efficiency of organic carbon in marine sediments, Nat Commun, 13, 7297, https://doi.org/10.1038/s41467-022-35112-9, 2022.

Cui, X., Bianchi, T. S., Savage, C., and Smith, R. W.: Organic carbon burial in fjords: Terrestrial versus marine inputs, Earth Planet Sci Lett, 451, 41–50, https://doi.org/https://doi.org/10.1016/j.epsl.2016.07.003, 2016.

Cui, X., Mucci, A., Bianchi, T. S., He, D., Vaughn, D., Williams, E. K., Wang, C., Smeaton, C., Koziorowska-Makuch, K., Faust, J. C., Plante, A. F., and Rosenheim, B. E.: Global fjords as transitory reservoirs of labile organic carbon modulated by organo-mineral interactions, Sci Adv, 8, eadd0610, https://doi.org/10.1126/sciadv.add0610, 2022.

Diesing, M. and Smeaton, C.: Input data to spatially predict organic carbon stocks, carbon reactivity index and delta 13C in fjords around Stavanger, Norway, https://doi.org/10.5281/zenodo.18172827, January 2026.

Diesing, M., Kröger, S., Parker, R., Jenkins, C., Mason, C., and Weston, K.: Predicting the standing stock of organic carbon in surface sediments of the North–West European continental shelf, Biogeochemistry, 135, 183–200, https://doi.org/10.1007/s10533-017-0310-4, 2017.

Diesing, M., Paradis, S., Jensen, H., Thorsnes, T., Bjarnadóttir, L. R., and Knies, J.: Glacial troughs as centres of organic carbon accumulation on the Norwegian continental margin, Commun Earth Environ, 5, 327, https://doi.org/10.1038/s43247-024-01502-8, 2024a.

Diesing, M., Knies, J., Elvenes, S., and Bøe, R.: Kartlegging av organisk karbon i sjøbunnssedimenter i Stavanger kommune, NGU-Rapport, 2024.015, 2024b.

Diesing, M., Smeaton, C., Bjarnadóttir, L. R., and Thorsnes, T.: Hotspots and coldspots of seabed organic carbon on the Norwegian continental margin, Environ Res Commun, https://doi.org/10.1088/2515-7620/ae14bc, 2025.

Donato, D. C., Kauffman, J. B., Murdiyarso, D., Kurnianto, S., Stidham, M., and Kanninen, M.: Mangroves among the most carbon-rich forests in the tropics, Nature Geosci, 4, 293–297, 2011.

Duffield, C., Alve, E., Andersen, N., Andersen, T., Hess, S., and Strohmeier, T.: Spatial and temporal organic carbon burial along a fjord to coast transect: A case study from Western Norway, Holocene, 27, 1325–1339, https://doi.org/10.1177/0959683617690588, 2017.

Dürr, H. H., Laruelle, G. G., van Kempen, C. M., Slomp, C. P., Meybeck, M., and Middelkoop, H.: Worldwide Typology of Nearshore Coastal Systems: Defining the Estuarine Filter of River Inputs to the Oceans, Estuaries and Coasts, 34, 441–458, https://doi.org/10.1007/s12237-011-9381-y, 2011.

Elvenes, S., Bøe, R., Lepland, A., and Dolan, M.: Seabed sediments of Søre Sunnmøre, Norway, J Maps, 15, 686–696, https://doi.org/10.1080/17445647.2019.1659865, 2019.

Faust, J. C. and Knies, J.: Organic Matter Sources in North Atlantic Fjord Sediments, Geochemistry, Geophysics, Geosystems, 20, 2872–2885, https://doi.org/10.1029/2019GC008382, 2019.

Faust, J. C., Knies, J., Slagstad, T., Vogt, C., Milzer, G., and Giraudeau, J.: Geochemical composition of Trondheimsfjord surface sediments: Sources and spatial variability of marine and terrigenous components, Cont Shelf Res, 88, 61–71, https://doi.org/https://doi.org/10.1016/j.csr.2014.07.008, 2014.

https://doi.org/10.5194/egusphere-2026-108
Preprint. Discussion started: 15 January 2026
© Author(s) 2026. CC BY 4.0 License.

Flemming, B. W. and Delafontaine, M. T.: Mass physical properties of muddy intertidal sediments: some applications, misapplications and non-applications, Cont Shelf Res, 20, 1179–1197, https://doi.org/10.1016/S0278-4343(00)00018-2, 2000.

Graves, C. A., Benson, L., Aldridge, J., Austin, W. E. N., Dal Molin, F., Fonseca, V. G., Hicks, N., Hynes, C., Kröger, S., Lamb, P. D., Mason, C., Powell, C., Smeaton, C., Wexler, S. K., Woulds, C., and Parker, R.: Sedimentary carbon on the continental shelf: Emerging capabilities and research priorities for Blue Carbon, Front Mar Sci, 9, 926215, https://doi.org/10.3389/fmars.2022.926215, 2022.

Harris, D., Horwáth, W. R., and van Kessel, C.: Acid fumigation of soils to remove carbonates prior to total organic carbon or CARBON-13 isotopic analysis, Soil Science Society of America Journal, 65, 1853–1856, https://doi.org/https://doi.org/10.2136/sssaj2001.1853, 2001.

Hartigan, J. A. and Wong, M. A.: Algorithm AS 136: A K-Means Clustering Algorithm, J R Stat Soc Ser C Appl Stat, 28, 100–108, https://doi.org/10.2307/2346830, 1979.

Hemingway, J. D., Rothman, D. H., Rosengard, S. Z., and Galy, V. V: Technical note: An inverse method to relate organic carbon reactivity to isotope composition from serial oxidation, Biogeosciences, 14, 5099–5114, https://doi.org/10.5194/bg-14-5099-2017, 2017.

Heuvelink, G. B. M.: Uncertainty quantification of GlobalSoilMap products, in: GlobalSoilMap: Basis of the global spatial soil information system, edited by: Arrouays, D., McKenzie, N., Hempel, J., Richer de Forges, A., and McBratney, A. B., CRC Press, Boca Raton, 335–340, 2014.

Hourlier, D.: Thermal decomposition of calcium oxalate: beyond appearances, J Therm Anal Calorim, 136, 2221–2229, https://doi.org/10.1007/s10973-018-7888-1, 2019.

Howe, J. A., Austin, W. E. N., Forwick, M., Paetzel, M., Harland, R., and Cage, A. G.: Fjord systems and archives: a review, Geological Society, London, Special Publications, 344, 5–15, https://doi.org/10.1144/SP344.2, 2010.

Knies, J. and Martinez, P.: Organic matter sedimentation in the western Barents Sea region: Terrestrial and marine contribution based on isotopic composition and organic nitrogen content, Norwegian Journal of Geology, 89, 79–89, 2009.

Knies, J., Elvenes, S., and Bøe, R.: Sedimentasjonsmiljø og historisk utvikling i forurensingsstatus i sjøområdene i Stavanger kommune, NGU-Rapport, 2021.003, 84, 2021a.

Knies, J., Boitsov, S., Baeten, N. J., Elvenes, S., and Bøe, R.: Sedimentasjonsmiljø og historisk utvikling i forurensningsstatus i sjøområdene i kommunene Ålesund og Giske, NGU-Rapport, 2021.018, 67, 2021b.

Knies, J., Boitsov, S., Elvenes, S., and Bøe, R.: Sedimentasjonsmiljø og historisk utvikling i forurensningsstatus i sjøområde i kommunene Skjervøy, Kvænangen, og Nordreisa, NGU-Rapport, 2022.016, 64, 2022.

Knies, J., Boitsov, S., Elvenes, S., and Bøe, R.: Sedimentasjonsmiljø og historisk utvikling i forurensningsstatus i kommunene Sveio, Bømlo, Stord, Fitjar, Tysnes og Austevoll i Sunnhordland, NGU-Rapport, 2024.017, 67, 2024.

https://doi.org/10.5194/egusphere-2026-108
Preprint. Discussion started: 15 January 2026
© Author(s) 2026. CC BY 4.0 License.

Koziorowska, K., Kuliński, K., and Pempkowiak, J.: Comparison of the burial rate estimation methods of organic and inorganic carbon and quantification of carbon burial in two high Arctic fjords, Oceanologia, 60, 405–418, https://doi.org/10.1016/j.oceano.2018.02.005, 2018.

Laruelle, G. G., Rosentreter, J. A., and Regnier, P.: Extrapolation-Based Regionalized Re-evaluation of the Global Estuarine Surface Area, Estuaries and Coasts, 48, 34, https://doi.org/10.1007/s12237-024-01463-3, 2024.

Lepland, A., Jensen, H. K. B., Plassen, L., and Longva, O.: Forurensningsstatus i sjøbunnssedimenter i Astafjordområdet/Sør-Troms, NGU-Rapport, 2012.002, 37, 2012.

Meinshausen, N.: Quantile Regression Forests, Journal of Machine Learning Research, 7, 983–999, 2006.

Meyer, H. and Pebesma, E.: Predicting into unknown space? Estimating the area of applicability of spatial prediction models, Methods Ecol Evol, 12, 1620–1633, https://doi.org/10.1111/2041-210X.13650, 2021.

Meyer, H. and Pebesma, E.: Machine learning-based global maps of ecological variables and the challenge of assessing them, Nat Commun, 13, 2208, https://doi.org/10.1038/s41467-022-29838-9, 2022.

Meyer, H., Reudenbach, C., Hengl, T., Katurji, M., and Nauss, T.: Improving performance of spatio-temporal machine learning models using forward feature selection and target-oriented validation, Environmental Modelling & Software, 101, 1–9, https://doi.org/https://doi.org/10.1016/j.envsoft.2017.12.001, 2018.

Murray, N. J., Phinn, S. R., DeWitt, M., Ferrari, R., Johnston, R., Lyons, M. B., Clinton, N., Thau, D., and Fuller, R. A.: The global distribution and trajectory of tidal flats, Nature, 565, 222–225, https://doi.org/10.1038/s41586-018-0805-8, 2019.

NGU: Classification of Sediments Based on Grain Size Composition (Folk, 1954, Modified), 2019a.

NGU: Sedimentary Environment, 2019b.

Placitu, S., van de Velde, S. J., Hylén, A., Hall, P. O. J., Robertson, E. K., Eriksson, M., Leermakers, M., Mehta, N., and Bonneville, S.: Limited Organic Carbon Burial by the Rusty Carbon Sink in Swedish Fjord Sediments, J Geophys Res Biogeosci, 129, e2024JG008277, https://doi.org/https://doi.org/10.1029/2024JG008277, 2024.

Rosenheim, B. E., Santoro, J. A., Gunter, M., and Domack, E. W.: Improving Antarctic Sediment 14C Dating Using Ramped Pyrolysis: An Example from the Hugo Island Trough, Radiocarbon, 55, 115–126, https://doi.org/DOI: 10.2458/azu_js_rc.v55i1.16234, 2013.

Smeaton, C. and Austin, W. E. N.: Sources, Sinks, and Subsidies: Terrestrial Carbon Storage in Mid-latitude Fjords, J Geophys Res Biogeosci, 122, 2754–2768, https://doi.org/https://doi.org/10.1002/2017JG003952, 2017.

Smeaton, C. and Austin, W. E. N.: Where's the Carbon: Exploring the Spatial Heterogeneity of Sedimentary Carbon in Mid-Latitude Fjords, Front Earth Sci (Lausanne), 7, 269, https://doi.org/10.3389/feart.2019.00269, 2019.

Smeaton, C. and Austin, W. E. N.: Quality Not Quantity: Prioritizing the Management of Sedimentary Organic Matter Across Continental Shelf Seas, Geophys Res Lett, 49, e2021GL097481, https://doi.org/10.1029/2021GL097481, 2022a.

Smeaton, C. and Austin, W. E. N.: Understanding the Role of Terrestrial and Marine Carbon in the Mid-Latitude Fjords of Scotland, Global Biogeochem Cycles, 36, e2022GB007434, https://doi.org/https://doi.org/10.1029/2022GB007434, 2022b.

https://doi.org/10.5194/egusphere-2026-108
Preprint. Discussion started: 15 January 2026
© Author(s) 2026. CC BY 4.0 License.

Smeaton, C., Austin, W. E. N., Davies, A. L., Baltzer, A., Howe, J. A., and Baxter, J. M.: Scotland's forgotten carbon: a national assessment of mid-latitude fjord sedimentary carbon stocks, Biogeosciences, 14, 5663–5674, https://doi.org/10.5194/bg-14-5663-2017, 2017.

Smeaton, C., Yang, H., and Austin, W. E. N.: Carbon burial in the mid-latitude fjords of Scotland, Mar Geol, 441, 106618, https://doi.org/https://doi.org/10.1016/j.margeo.2021.106618, 2021.

Smith, R. W., Bianchi, T. S., Allison, M., Savage, C., and Galy, V.: High rates of organic carbon burial in fjord sediments globally, Nat Geosci, 8, 450–453, https://doi.org/10.1038/NGEO2421, 2015.

Syvitski, J. P. M., Burrell, D. C., and Skei, J. M.: Fjords and Their Study, in: Fjords: Processes and Products, edited by: Syvitski, J. P. M., Burrell, D. C., and Skei, J. M., Springer New York, New York, NY, 3–17, https://doi.org/10.1007/978-1-4612-4632-9_1, 1987.

Thornton, S. F. and McManus, J.: Application of Organic Carbon and Nitrogen Stable Isotope and C/N Ratios as Source Indicators of Organic Matter Provenance in Estuarine Systems: Evidence from the Tay Estuary, Scotland, Estuar Coast Shelf Sci, 38, 219–233, https://doi.org/https://doi.org/10.1006/ecss.1994.1015, 1994.

Wadoux, A. M. J.-C., Heuvelink, G. B. M., de Bruin, S., and Brus, D. J.: Spatial cross-validation is not the right way to evaluate map accuracy, Ecol Modell, 457, 109692, https://doi.org/10.1016/j.ecolmodel.2021.109692, 2021.

Watts, E. G., Hylén, A., Hall, P. O. J., Eriksson, M., Robertson, E. K., Kenney, W. F., and Bianchi, T. S.: Burial of Organic Carbon in Swedish Fjord Sediments: Highlighting the Importance of Sediment Accumulation Rate in Relation to Fjord Redox Conditions, J Geophys Res Biogeosci, 129, e2023JG007978, https://doi.org/https://doi.org/10.1029/2023JG007978, 2024.

Watts, E. G., Zautcke, K., Santos, I., Smeaton, C., Ljungberg, W., Cheung, H. L. S., Bonaglia, S., Politi, T., Liu, Z., and Bianchi, T. S.: Efficient Burial of Labile Organic Carbon in Sediments of Oxygenated Icelandic Fjords, Estuaries and Coasts, 48, 167, https://doi.org/10.1007/s12237-025-01582-5, 2025.

Winkelmann, D. and Knies, J.: Recent distribution and accumulation of organic carbon on the continental margin west off Spitsbergen, Geochemistry, Geophysics, Geosystems, 6, https://doi.org/https://doi.org/10.1029/2005GC000916, 2005.

Włodarska-Kowalczuk, M., Mazurkiewicz, M., Górska, B., Michel, L. N., Jankowska, E., and Zaborska, A.: Organic Carbon Origin, Benthic Faunal Consumption, and Burial in Sediments of Northern Atlantic and Arctic Fjords (60–81°N), J Geophys Res Biogeosci, 124, 3737–3751, https://doi.org/https://doi.org/10.1029/2019JG005140, 2019.

https://doi.org/10.5194/egusphere-2026-108
Preprint. Discussion started: 15 January 2026
© Author(s) 2026. CC BY 4.0 License.

Table 1. Absolute and relative area occupied by substrate types

Substrate type	Area (km^2)	Area (% of total)
Mud	30.37	12.0
Sandy mud	34.54	13.6
Muddy sand	11.72	4.6
Sand	6.85	2.7
Gravelly sandy mud	14.53	5.7
Gravelly muddy sand	5.31	2.1
Gravelly sand	8.52	3.4
Sandy gravel	1.12	0.4
Sand, gravel, cobbles and boulders	30.14	11.9
Gravel and cobbles	0.70	0.3
Sand, gravel and cobbles	10.10	4.0
Gravel, cobbles and boulders	2.34	0.9
Cobbles and boulders	0.07	0.0
Mud and sand with gravel, cobbles and boulders	12.62	5.0
Mud/sand with cobbles/boulders	0.01	0.0
Cobbles/boulders covered by mud/sand	0.07	0.0
Thin or discontinuous sediment cover on bedrock	84.02	33.2

690 **Table 2. Percentiles calculated for the 28 $OCAR_{10}$ values in g C m^{-2} yr^{-1} compiled in this study. P5 – 5th percentile; Q1 – 1st quartile; Q3 – 3rd quartile; P95 – 95th percentile.**

5% (P5)	25% (Q1)	50% (Median)	75% (Q3)	95% (P95)
18.4	25.7	40.5	60.1	82.3

https://doi.org/10.5194/egusphere-2026-108
Preprint. Discussion started: 15 January 2026
© Author(s) 2026. CC BY 4.0 License.

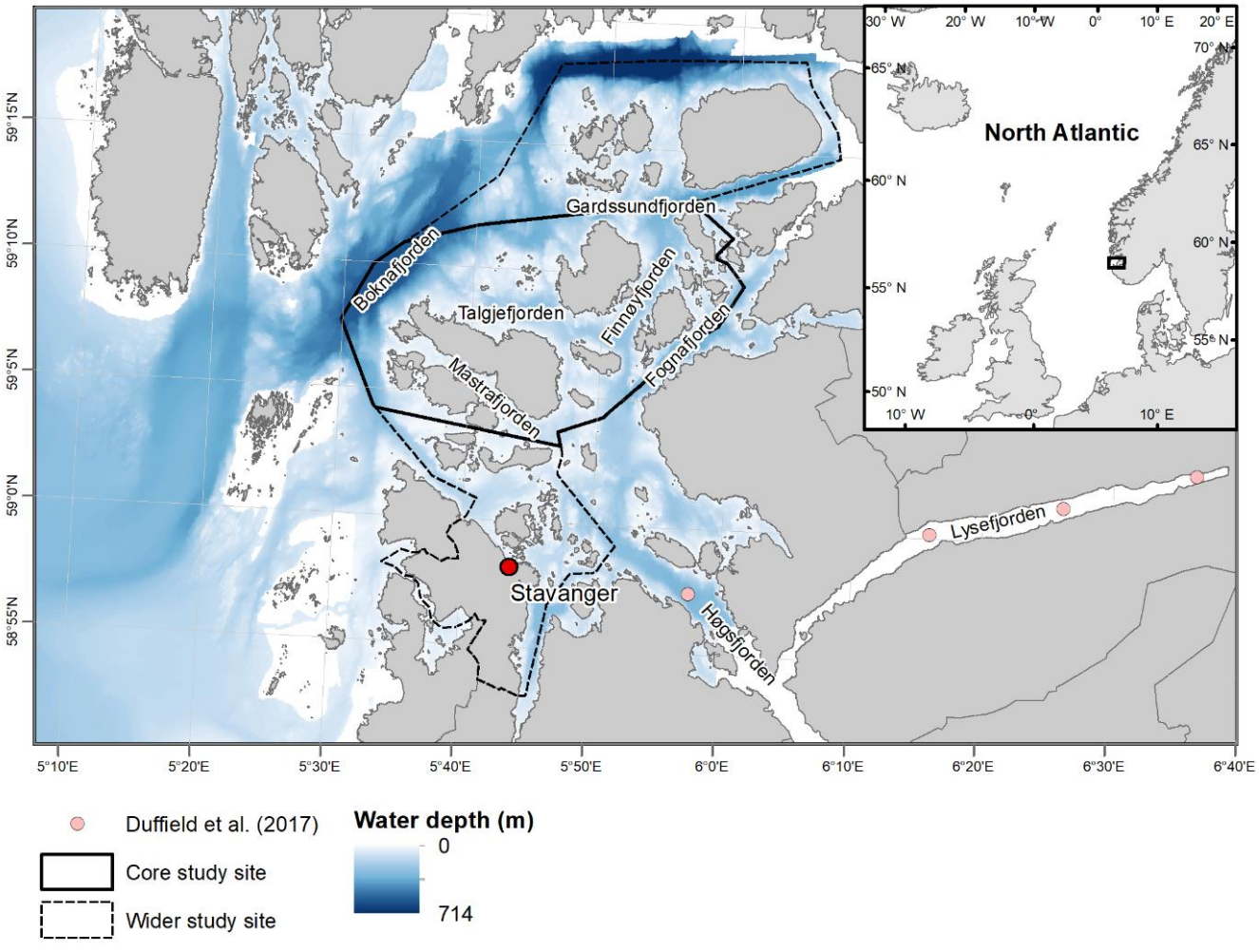

Figure 1. Overview of the wider and core study sites. Also shown are coring locations from Duffield et al. (2017). Bathymetry data available from Kartverket (hoydedata.no). White areas indicate no bathymetry data. The inset shows the location of the study site in northwest Europe (black rectangle).

https://doi.org/10.5194/egusphere-2026-108
Preprint. Discussion started: 15 January 2026
© Author(s) 2026. CC BY 4.0 License.

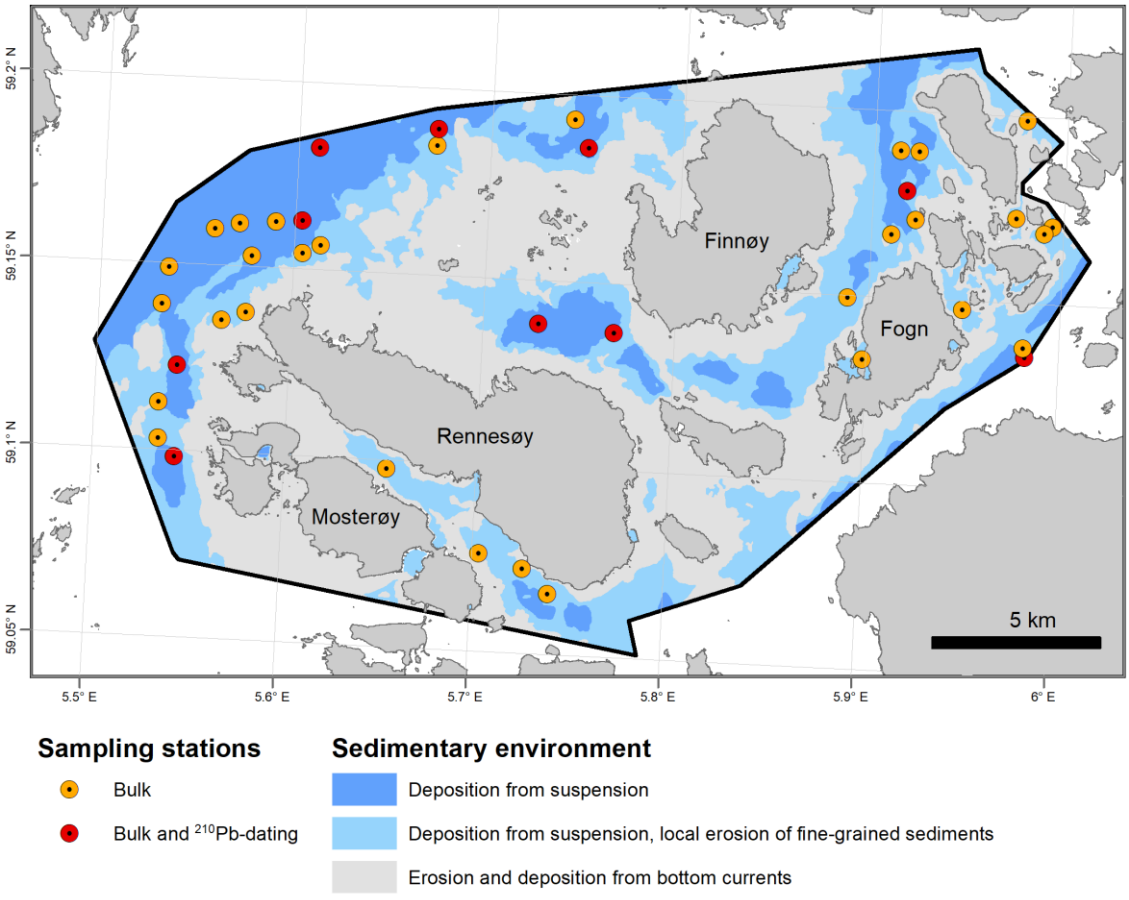

Figure 2. Overview of sampling stations. Bulk samples of the upper 10 cm of the sediment were collected at 40 stations. Multi cores for ^{210}Pb-dating were collected at a subset of the bulk sampling stations.

700

https://doi.org/10.5194/egusphere-2026-108
Preprint. Discussion started: 15 January 2026
© Author(s) 2026. CC BY 4.0 License.

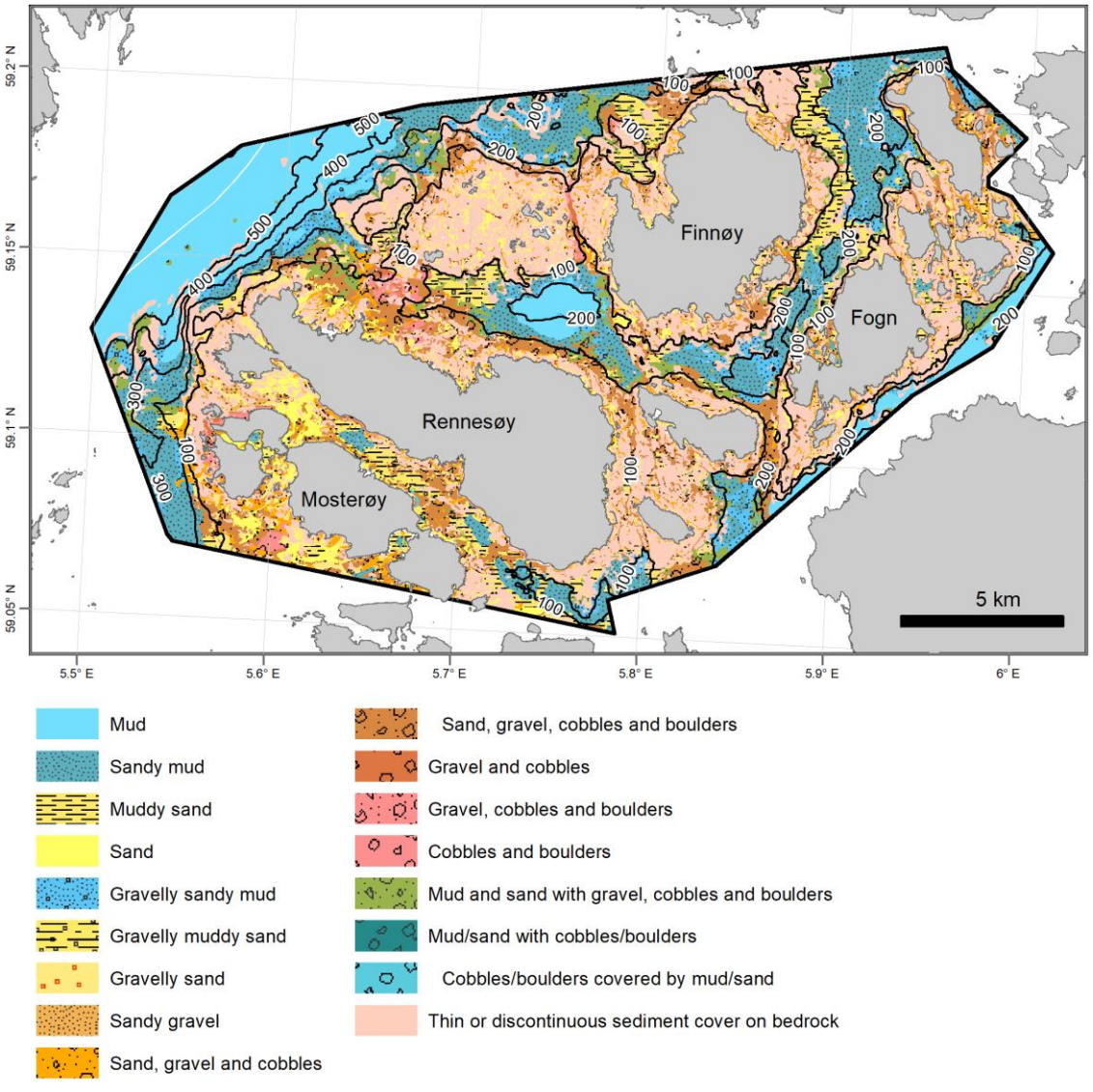

Figure 3. Substrate types in the core study site. Isobaths are shown in 100 m-intervals.

https://doi.org/10.5194/egusphere-2026-108
Preprint. Discussion started: 15 January 2026
© Author(s) 2026. CC BY 4.0 License.

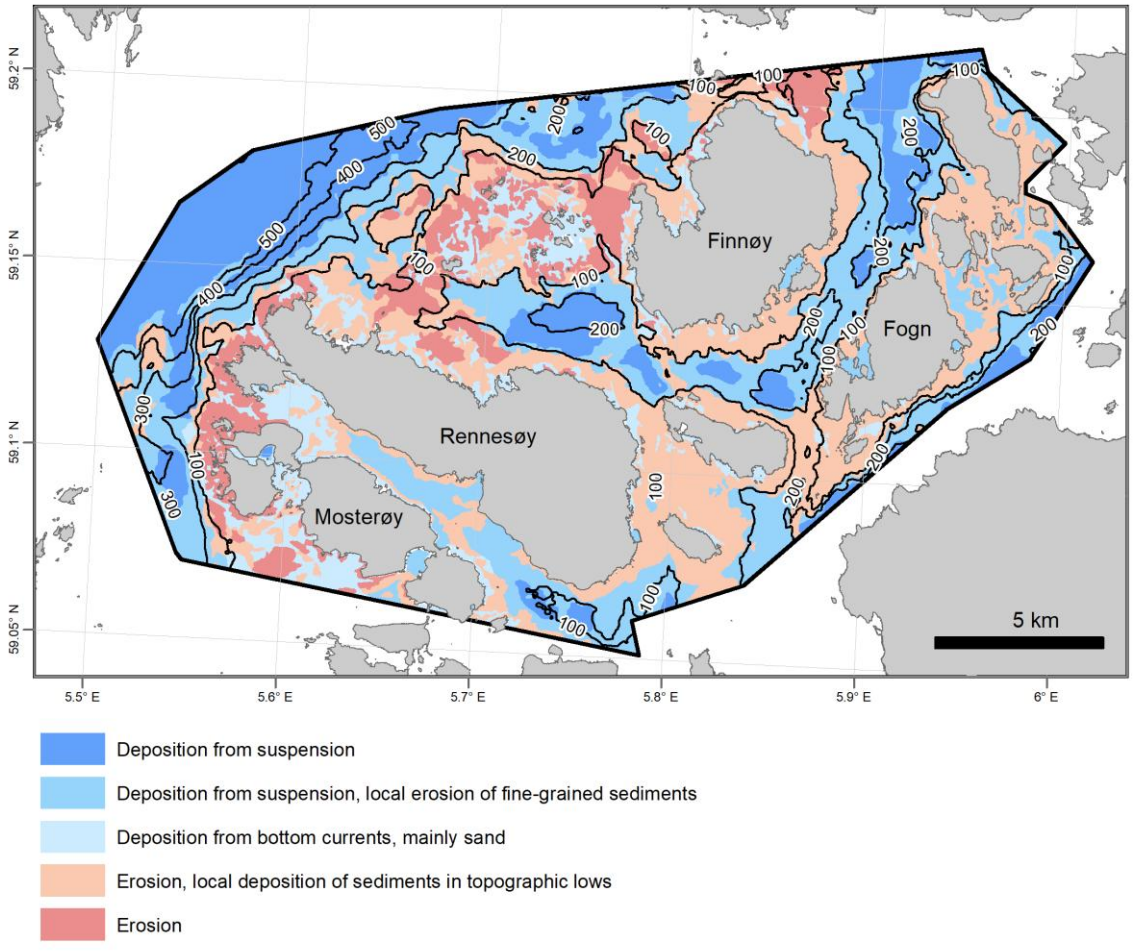

Figure 4. Sedimentary environment in the core study site. Isobaths are shown in 100 m-intervals.

https://doi.org/10.5194/egusphere-2026-108
Preprint. Discussion started: 15 January 2026
© Author(s) 2026. CC BY 4.0 License.

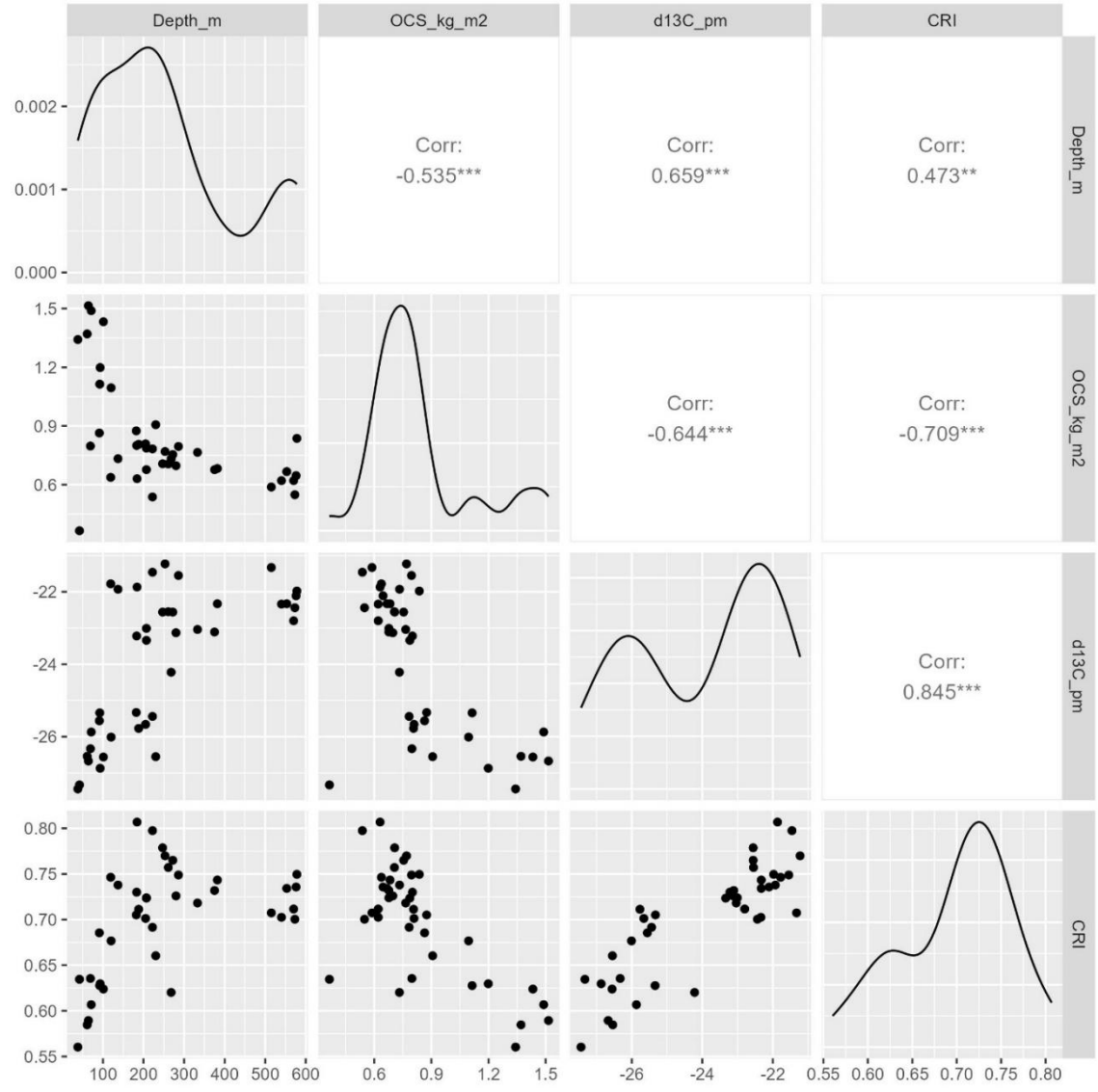

Figure 5. Generalised pairs plot showing the relationships between the response variables and water depth. Corr: Pearson product moment correlation coefficient. Asterisks indicate p-values. **: p < 0.01 and ***: p < 0.001.

710

https://doi.org/10.5194/egusphere-2026-108
Preprint. Discussion started: 15 January 2026
© Author(s) 2026. CC BY 4.0 License.

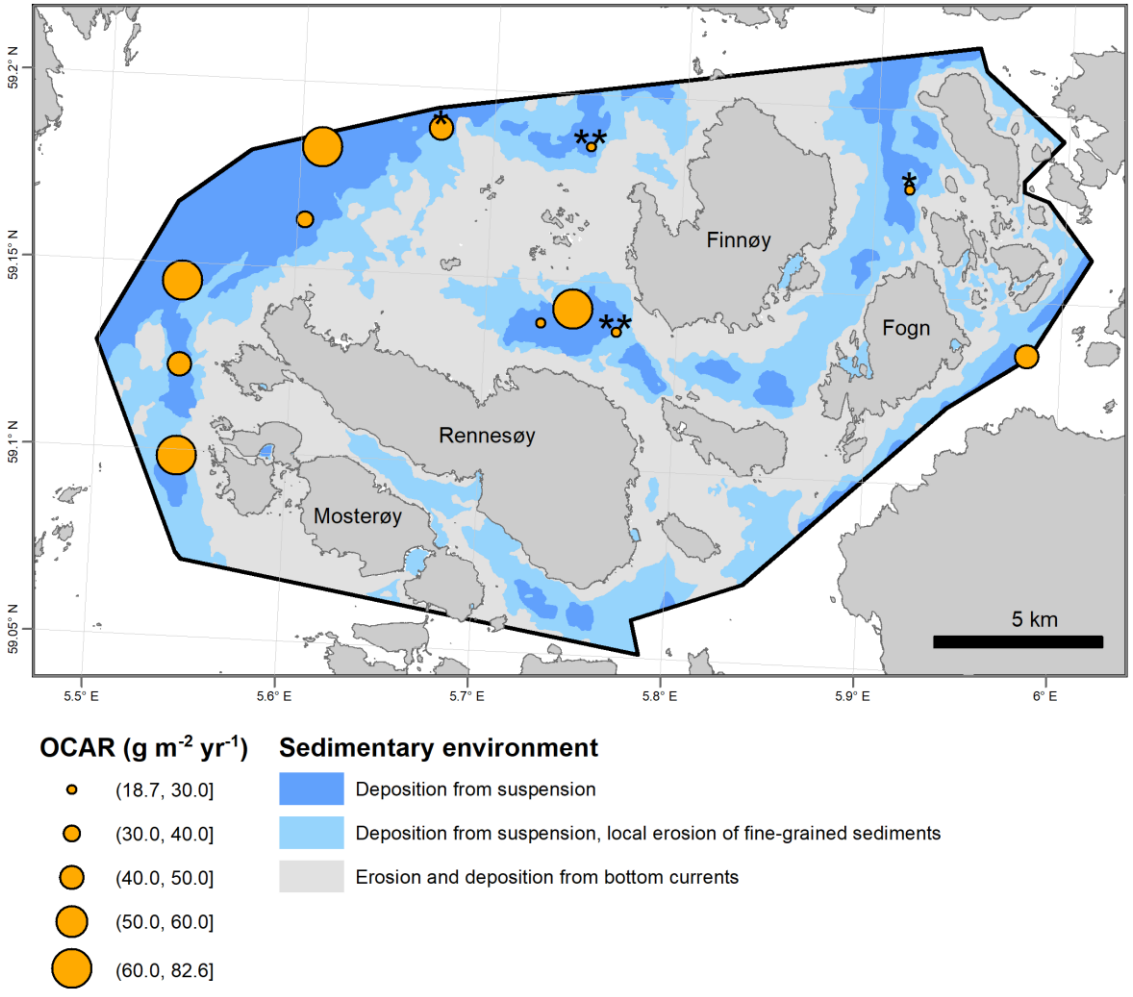

Figure 6. Organic carbon accumulation rates ($OCAR_{10}$). Cores were collected within areas mapped as deposition from suspension (see Figure 4). One asterisk (*) indicates cores potentially affected by sediment mixing and two asterisks (**) indicate cores affected by sediment mixing.

715

https://doi.org/10.5194/egusphere-2026-108
Preprint. Discussion started: 15 January 2026
© Author(s) 2026. CC BY 4.0 License.

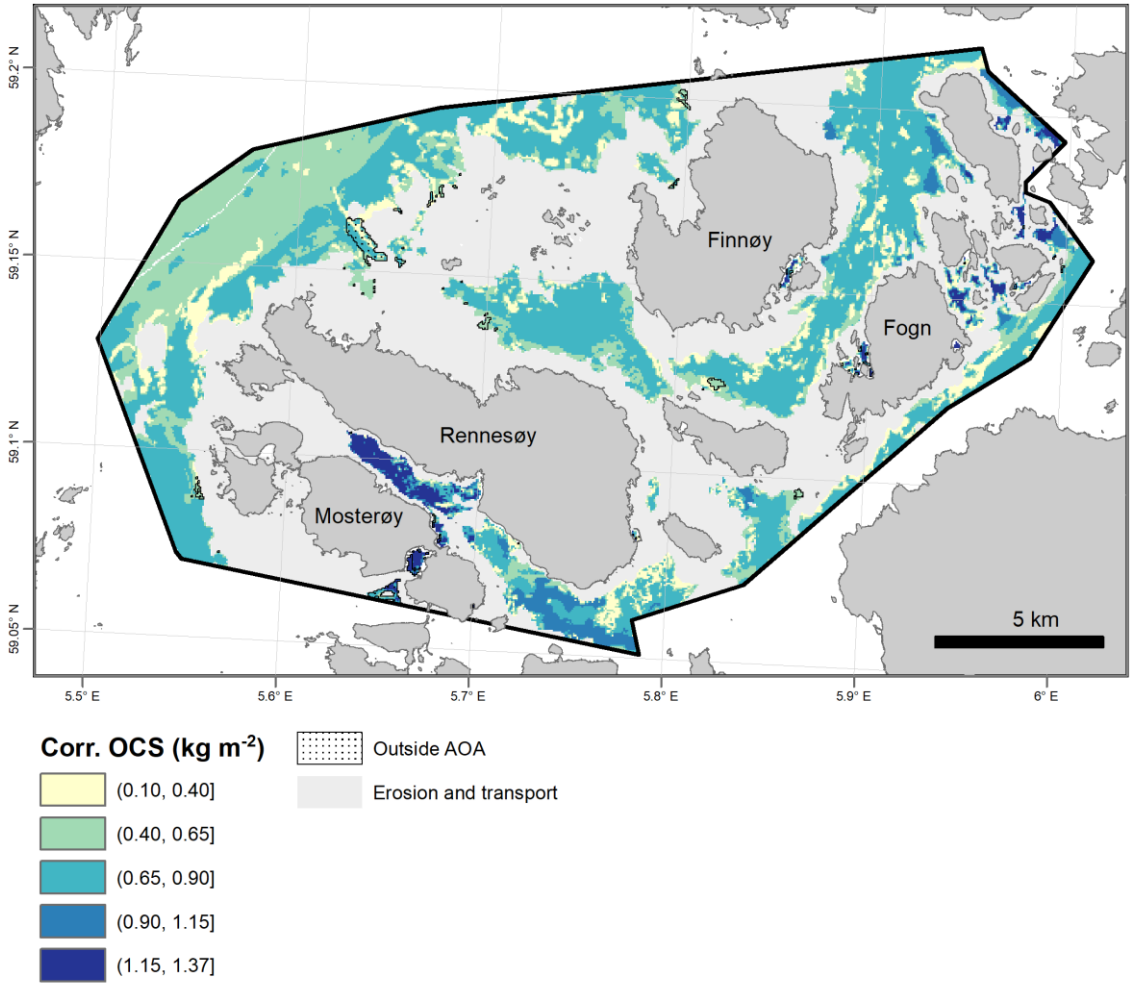

Figure 7. Corrected organic carbon stocks (OCS) of the upper 10 cm of the sediment. Predictions outside the area of applicability (AOA) of the model are shown as well.

https://doi.org/10.5194/egusphere-2026-108
Preprint. Discussion started: 15 January 2026
© Author(s) 2026. CC BY 4.0 License.

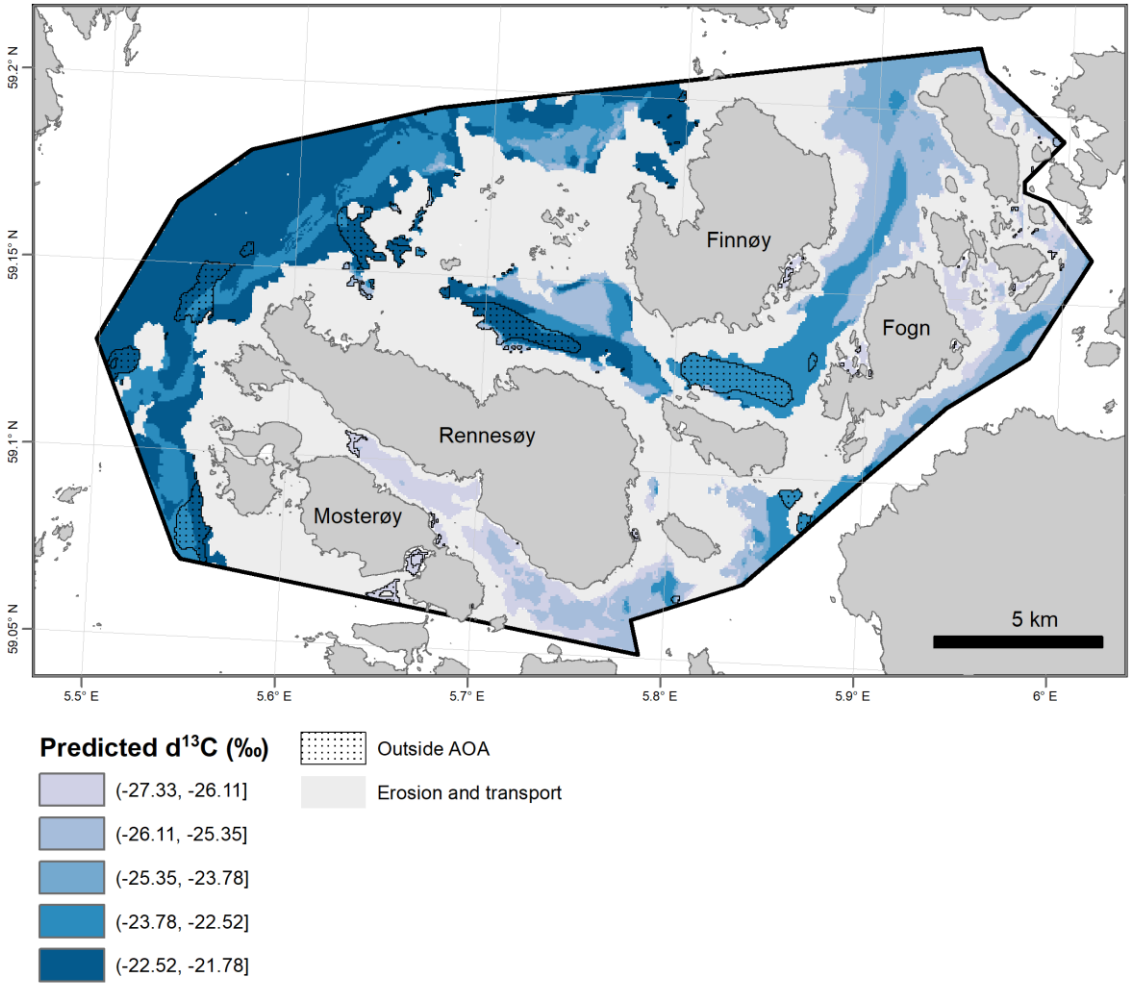

720

Figure 8. Stable carbon isotope ($d^{13}C$) values. Predictions outside the area of applicability (AOA) of the model are shown as well.

https://doi.org/10.5194/egusphere-2026-108
Preprint. Discussion started: 15 January 2026
© Author(s) 2026. CC BY 4.0 License.

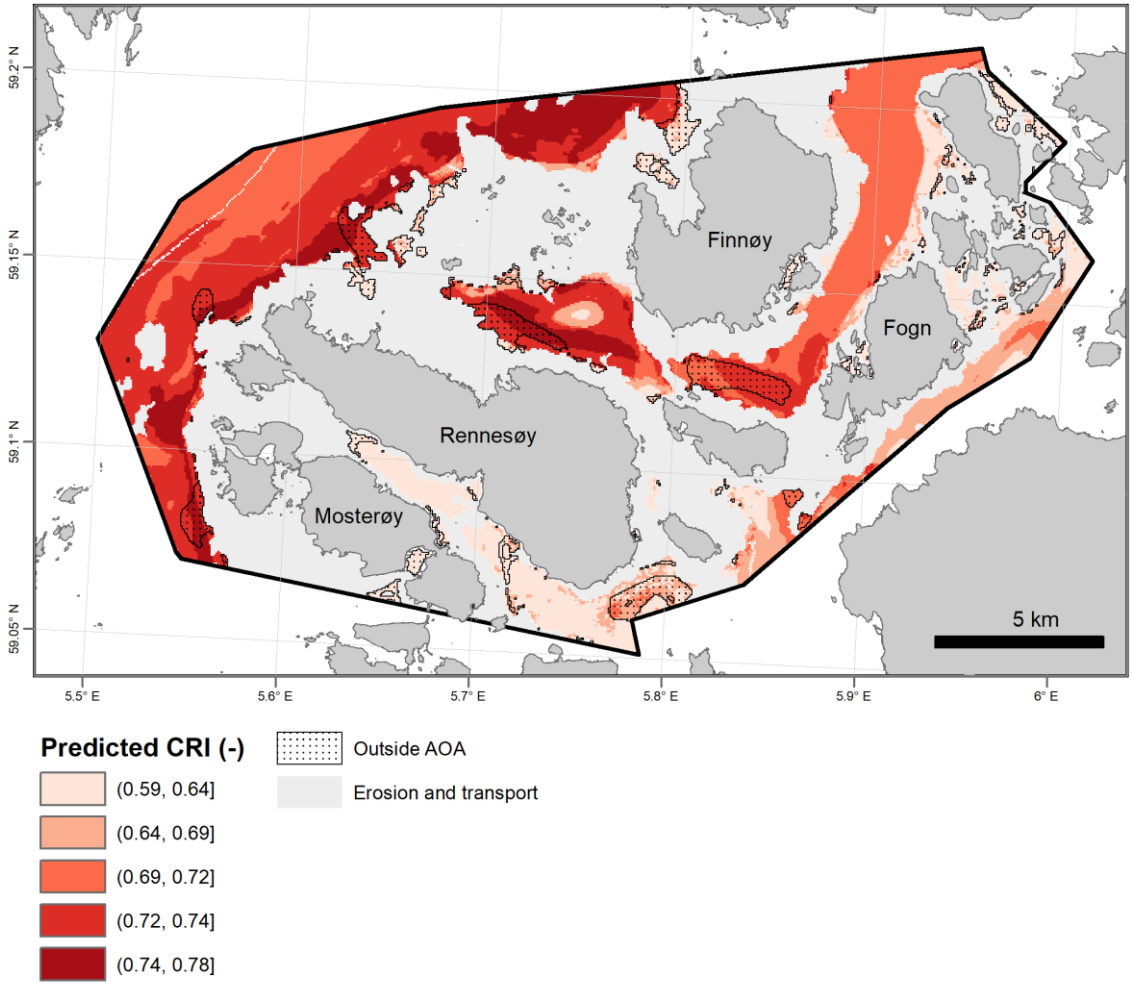

Figure 9. Carbon reactivity index (CRI). Predictions outside the area of applicability of the model are shown as well.

725

https://doi.org/10.5194/egusphere-2026-108
Preprint. Discussion started: 15 January 2026
© Author(s) 2026. CC BY 4.0 License.

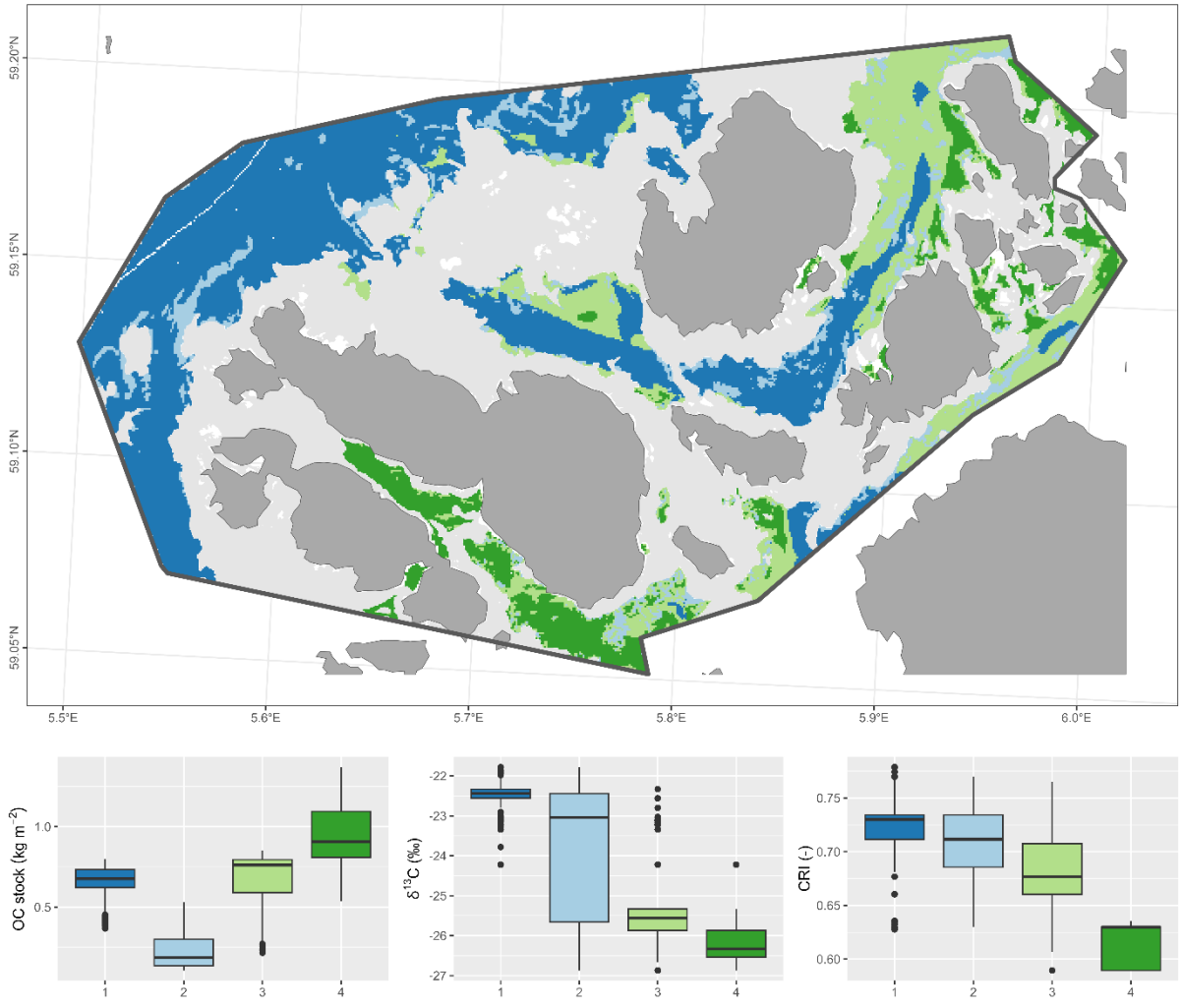

Figure 10. Regionalisation with four clusters. Boxplots of the variables used for clustering show the properties of the clusters. The thick horizontal line of the boxplots is the median, the ends of the box are the upper (Q3) and lower (Q1) quartiles, defining the interquartile range (IQR), the whiskers show the range of values within Q3 + 1.5 × IQR to Q1 - 1.5 × IQR, representing the highest and lowest values, excluding outliers and outliers are the dots beyond the whiskers.